

# **Phosphorylation of Dentin Matrix Protein 1 and Phosphophoryn**

by

Yuanyuan Duan

Submitted to the Graduate Faculty of  
University of Pittsburgh in partial fulfillment  
of the requirements for the degree of  
Master of Science

University of Pittsburgh

2009

UNIVERSITY OF PITTSBURGH

School of Medicine

This thesis was presented

by

Yuanyuan Duan

It was defended on

[Jun 23rd, 2009]

and approved by

[Charles Sfeir, Assoc. Professor, Dept. of Oral Biology]

[Michael Cascio, Assoc. Professor, Dept. of Molecular Genetics and Biochemistry]

[Peijun Zhang, Assis. Professor, Dept. of Structural biology]

[Thesis Director]: [Billy W Day, Professor, Dept.of Pharmaceutical Sciences]

Copyright © by Yuanyuan Duan

2009

## **Phosphorylation of Dentin Matrix Protein 1 and Phosphophoryn**

Yuanyuan Duan

University of Pittsburgh, 2009

### **ABSTRACT**

Yuanyuan Duan

University of Pittsburgh, 2009

Biom mineralization, one of the most widespread processes in nature, uses polyanionic proteins to direct oriented crystal growth. In bone and dentin, this process is under precise control of the collagen template and the noncollagenous acidic phosphoproteins. These phosphoproteins function differently depending on their sizes and level of phosphorylation.

The goal of this research is to investigate the *in vitro* phosphorylation as well as the phosphorylation in mammalian cells of two highly phosphorylated bone/dentin extracellular matrix proteins: dentin phosphophoryn (DPP) and dentin matrix protein 1 (DMP1). This data will be important to the general hypothesis, that the phosphorylation of non-collagenous proteins play a significant role in matrix mediated mineralization.

Our data shows that the *in vitro* phosphorylation of DPP and DMP1 could be optimized by adjusting the phosphorylation reaction time, calcium concentration, and protein modification by assessing various forms (with or without the C or N terminal end). Following the *in vitro* phosphorylation, mass spectrometry analysis was used to identify the sites of phosphorylation. In addition, to identify the kinases involved in phosphorylating DMP1, cell lysates from cells that

have (MC3T3) and do not have (NIH3T3) the ability to mineralize their matrix and were isolated and analyzed by zymogram. Casein kinase II catalytic subunit was identified in addition to potential novel kinases responsible for DMP1 phosphorylation, some possible novel kinases for DMP1 were discovered by mass spectrometry.

The second goal of this research is to assess if cells that have the ability to form a mineralized matrix will possess specialized kinases that can phosphorylate these highly phosphorylated and acidic proteins. To achieve this goal we over-expressed and purified DMP1 from two cell types: 1) cells that have the ability to mineralize their matrix and 2) cells that do not possess the ability to mineralize their matrix. The purified proteins were then analyzed by SDS-PAGE and mass spectrometry to quantify and determine the sites of phosphorylation.

This study has expanded our knowledge on the mechanisms involved in the phosphorylation of DPP and DMP1 and provided the parameters to start assessing the role of phosphorylation on tissue mineralization.

## TABLE OF CONTENTS

<b>ACKNOWLEDGEMENTS .....</b>	<b>XII</b>
<b>NOMENCLATURE .....</b>	<b>XIII</b>
<b>1.0 INTRODUCTION.....</b>	<b>1</b>
<b>1.1 OVERVIEW .....</b>	<b>1</b>
<b>1.2 MINERAL FORMATION AND EXTRACELLULAR MATRIX .....</b>	<b>3</b>
<b>1.3 EXTRACELLULAR MATRIX COLLAGEN .....</b>	<b>4</b>
<b>1.4 NON-COLLAGENOUS PROTEINS.....</b>	<b>4</b>
<b>1.5 SIBLING PROTEINS.....</b>	<b>6</b>
<b>1.5.1 Dentin Phosphophoryn (DPP) .....</b>	<b>7</b>
<b>1.5.2 Dentin Matrix Protein 1 (DMP1) .....</b>	<b>9</b>
<b>1.6 PHOSPHORYLATION BY EUKARYOTIC PROTEIN KINASES.....</b>	<b>12</b>
<b>2.0 HYPOTHESIS .....</b>	<b>14</b>
<b>3.0 MATERIAL AND METHODS .....</b>	<b>15</b>
<b>3.1 REAGENTS AND MATERIALS.....</b>	<b>15</b>
<b>3.2 RECOMBINANT PROTEIN PURIFICATION .....</b>	<b>15</b>
<b>3.2.1 Constructs and mutation .....</b>	<b>15</b>
<b>3.2.2 Recombinant protein purification .....</b>	<b>17</b>
<b>3.3 TISSUE CLUTURE OF CELLS .....</b>	<b>17</b>

3.4	DMP1 PURIFICATION FROM CELLS.....	18
3.5	CELL CYTOSOLIC AND MEMBRANOUS FRACTIONS PREPARATION .....	19
3.6	<i>IN VITRO</i> PHOSPHORYLATION.....	20
3.6.1	<i>In vitro</i> phosphorylation by CKI and CKII .....	20
3.6.2	<i>In vitro</i> phosphorylation by cell fractions .....	21
3.6.3	Phosphorylation quantification by scintillation counter .....	21
3.6.4	Phosphorylation detection by SDS-Gel.....	22
3.7	MASS SPECTROMETRY .....	23
3.7.1	In gel digestion .....	23
3.7.2	In solution digestion.....	24
3.7.3	MALDI-TOF MS.....	24
3.7.4	LC-ESI MS.....	25
3.8	ZYMOGRAM .....	25
3.8.1	Detection of the kinase activity after 1-Dimension SDS-PAGE .....	25
3.8.2	Kinase identification using mass spectrometry.....	26
4.0	RESULTS AND DISCUSSION .....	27
4.1	MASS SPECTROMETRY OF PP.....	27
4.2	MASS SPECTROMETRY OF DMP1 .....	30
4.3	<i>IN VITRO</i> PHOSPHORYLATION OF PP .....	33
4.4	<i>IN VITRO</i> PHOSPHORYLATION OF DMP1 .....	37
4.5	ZYMOGRAM .....	45
4.6	MAMMALIAN CELL DERIVED DMP1 .....	53

<b>4.7</b>	<b>DISCUSSION.....</b>	<b>59</b>
<b>4.8</b>	<b>SUMMARY AND FUTURE RESEARCH .....</b>	<b>61</b>
	<b>BIBLIOGRAPHY .....</b>	<b>63</b>



## LIST OF TABLES

Table 1 Major non-collagenous proteins in bone and dentin .....	5
Table 2 Post-translational modifications of Sibling Proteins [18].....	7
Table 3 Cycles of PCR .....	16
Table 4 List of enzymes and chemicals that might cleave rPP.....	28
Table 5 Phospho-peptide of in vitro phosphorylated cDMP1 detected by MS .....	43
Table 6 List of kinases found in MC3T3 cell lysis' zymogram bands (37 and 40KD) .....	49
Table 7 List of kinases found in MDPC23 cell lysis' zymogram bands(37 and 40KD) .....	52

## LIST OF FIGURES

Figure 1. Osteogenesis(left) and odontogenesis(right) .....	2
Figure 2. Genomic organization of the mouse DSPP gene .....	8
Figure 3 Scheme of different forms of DPP .....	8
Figure 4 DMP1 is required for both osteogenesis and odontogenesis .....	10
Figure 5 DMP1 is cleaved into 2 fragments .....	11
Figure 6 Scheme of different forms of DMP1 .....	11
Figure 7 Strategy for subcellular fraction.....	20
Figure 8 rPP cleaved by enzymes and chemicals .....	29
Figure 9 cDMP1 digested by trypsin .....	31
Figure 10 cDMP1 digested by AspN .....	32
Figure 11 Comparison of in vitro phosphorylation of different PP forms .....	34
Figure 12 In vitro phosphorylation of different PP forms by CKI .....	35
Figure 13 Quantified comparison of in vitro phosphorylation of different PP forms by CKI .....	35
Figure 14 Comparison of rPP phosphorylated by different enzymes .....	36
Figure 15 In vitro phosphorylation of rPP by different time scale .....	36
Figure 16 In vitro phosphorylation of cDMP1 at different temperatures .....	38
Figure 17 In vitro phosphorylation of cDMP1 by CKI and CKII .....	39

Figure 18 In vitro phosphorylation of cDMP1 at different time points .....	39
Figure 19 In vitro phosphorylation of cDMP1 with different Ca <sup>2+</sup> (upper) or Mg <sup>2+</sup> concentration .....	40
Figure 20 MS of phosphorylated cDMP1 (phospho-peptides circled) .....	42
Figure 21 Phosphor-peptide 3071(1023.85*3) by LTQ-ESI MS <sup>n</sup> .....	44
Figure 22 Phospho-peptide 2510(838.32*3) by LCQ-ESI MS <sup>2</sup> .....	45
Figure 23 cDMP1 phosphorylated by cellular fractions .....	47
Figure 24 fDMP1 zymogram bands.....	48
Figure 25 MS/MS spectrum of peptide from CKII subunit alpha: VYAEVNSLR.....	50
Figure 26 MS/MS spectrum of peptide from CKII subunit alpha: HLVSPEALDLLDK .....	51
Figure 27 U2OS derived fDMP1 purified by ion exchange.....	54
Figure 28 MC3T3/ HEK293 derived DMP1 purified by ion exchange column .....	54
Figure 29 293 derived fDMP1 digested by trypsin. Coverage:31%.....	55
Figure 30 U2OS derived fDMP1 digested by trypsin. Coverage:30% .....	56
Figure 31 U2OS derived fDMP1 digested by AspN. Coverage: 36%.....	57
Figure 32 MC3T3derived fDMP1 digested by Trypsin. Coverage:22% .....	58
Figure 33 MC3T3derived fDMP1 digested by AspN. Coverage: 19% .....	59

## ACKNOWLEDGEMENTS

I extend my very deepest and sincere gratitude to Dr. Charles Sfeir and Dr. Billy Day, my advisors. Thanks for giving me an opportunity to work on this project. The experiences that I have had while working with them were invaluable. Their scientific guidance, patience, support, willingness to share and help have led me complete my graduate studies.

I express my appreciation to Dr. Michael Cascio and Dr. Peijun Zhang for their advice and for being on my committee.

I am thankful to all the people from whom I have learned techniques and procedures over the years: Jinhua Li, Dr. Guy Uechi, and Linda Zhang.

Thanks to Dr. Brian Hood and Dr. Emanuel Schreiber for their help on LC-MS.

Thanks to Diane Turner and Michele Leahy for always being helpful.

Finally, I would like to express my gratitude to my family, for being there every time I needed them.

## NOMENCLATURE

CID: Collision-induced dissociation

CKI: Casein Kinase I

CKII: Casein Kinase II

DSPP: Dentin sialophosphoprotein

DPP: Dentin phosphophoryn

DSP: Dentin sialoprotein

DGP: Dentin glycoprotein

DMP1: Dentin matrix protein 1

ESI: Electro spray ionization

ETD: Electron transfer dissociation

MALDI: Matrix-assisted laser desorption/ionization

MS: Mass spectrometry

NCP: non-collagenous proteins

TCEP: Tris (2-carboxyethyl) phosphine

TOF: Time of Flight

IAA: Iodoacetamide

## **1.0 INTRODUCTION**

### **1.1 OVERVIEW**

Osteogenesis (the process of bone formation) and Odontogenesis (the formation and development of teeth) are very similar. During osteogenesis, the osteoblasts arise from the osteoprogenitor cells in the bone marrow; mature osteoblasts produce a layer of nonmineralized collagenous matrix, which is called osteoid layer. Odontoblasts arise from the dental mesenchymal cells and secrete nonmineralized collagenous pre-dentin layer. Osteoid layer and pre-dentin layer mineralize leading to formation of bone and dentin tissues, respectively (Figure 1). Mature bone and dentin are composed of 60% mineral, 30% organic matrix and 10% water (by weight); this organic matrix consists of 90% type I collagen and 10% non-collagenous proteins[1]. Formation of pre-dentin and osteoid and their transformation process to dentin and bone are highly controlled by the cells.

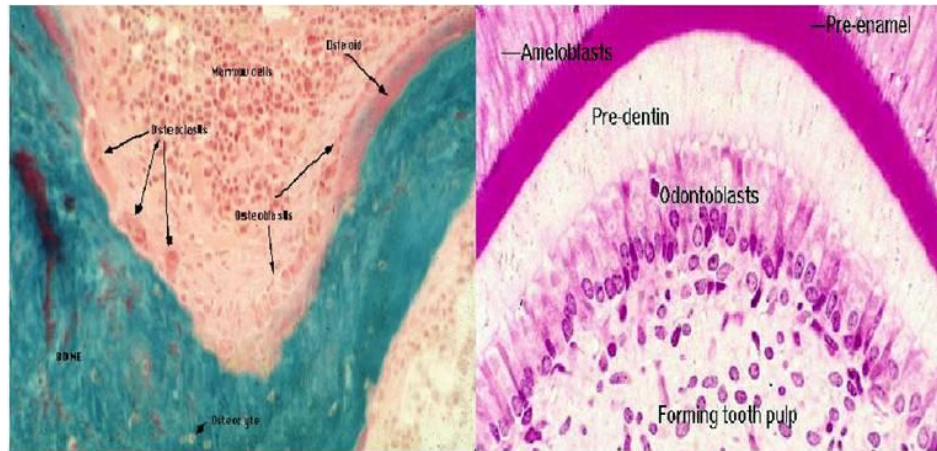


Figure 1. Osteogenesis(left) and odontogenesis(right)

During osteogenesis, the osteoblasts arise from the dental mesenchymal cells and secrete the osteoid layer. During odontogenesis, odontoblasts arise from the dental mesenchymal cells and secrete pre-dentin layer.

(from: [http://www.biyolojiegitim.yyu.edu.tr/k/ostblstm/pages/osteoblast\\_jpg.htm](http://www.biyolojiegitim.yyu.edu.tr/k/ostblstm/pages/osteoblast_jpg.htm). and <http://education.vetmed.vt.edu/Curriculum/VM8054/Labs/Lab17/Images/DIGL14.JPG>)

The biological control of mineralization requires regulation in time and space. This regulation involves extracellular organic matrices molecules which provide organized nucleation sites and entropic factors that control the nucleation and growth kinetics of crystal growth. Our knowledge of how the mineralization process is initiated and regulated is limited. However, the non-collagenous proteins (NCP) of bone/dentin are believed to play an important role in mineralization.

## 1.2 MINERAL FORMATION AND EXTRACELLULAR MATRIX

Bone, dentin and cartilage are all calcified tissues, they function both structurally and physiologically. Structurally, calcified tissues provide the rigid elements of bone and tooth. Physiologically, calcified tissues play an essential role in the regulation of ion' levels in body fluid by acting as storage for ions. The major ions that are primarily regulated by bone are calcium and phosphate. One of the areas of high interest in calcified tissue research is the biomineralization process in these hard tissues.

The major mineral in vertebrates hard tissues is calcium phosphate , in the form of calcium hydroxyapatite ( $\text{Ca}_{10}(\text{PO}_4)_6\text{OH}_2$ ) and amorphous calcium phosphate [2]. The body fluids are super-saturated in respect to calcium and phosphate, hence prone to spontaneous hydroxyapatite precipitation. Calcium phosphate precipitation is highly regulated by the cells, which prevent spontaneous precipitation in soft tissues and induce controlled mineral formation in bone and dentin; if the process is not properly regulated, the result could be too little or too much mineral-either of which can compromise health[3] .

The mineralization process in bone and dentin is regulated by cells. The cells produce an organic matrix rich in acidic macromolecules. This matrix controls all aspects of mineral formation, including crystal nucleation growth kinetics, crystal size, morphology and organization of the crystals in the tissue. There are two mechanism of nucleation: homogeneous and heterogeneous. Homogeneous nucleation is a process that involves only precursor solutions without any foreign material (such as proteins) while heterogeneous nucleation is a process with foreign material. For bone and dentin formation, it is believed that the mineralization occurs via heterogeneous nucleation process[4]. Many macromolecules (e.g. collagen, non-collagen proteins) play an essential role in the mineralization process. Collagen works as a structural



template whereas non-collagen proteins, acidic in nature and highly phosphorylated, strongly bind calcium[4] .

### **1.3 EXTRACELLULAR MATRIX COLLAGEN**

Calcification of bone and dentin requires an extracellular matrix (ECM). Type I collagen is the major extracellular matrix protein, providing structural template for bone/dentin formation. ECM of bone and dentin contain mainly type I collagen and very limited other fibrillar collagens. Type I collagen, the most abundant collagen in the human body, is the major matrix protein in both bone and dentin. It is packed as a 2-D quarter-staggered arrangement and a 3-D quasi-hexagonal assembly to construct the fibrillar matrix, providing structural scaffold [5]. Analysis suggests that the type I collagen and non-collagenous matrix provides a template of charged amino acids such as glutamic acid, aspartic acid, lysine, arginine, hydroxylysine and histidine. This template dictates mineral formation in vertebrate tissues[6]. As a scaffold and deposition space, type I collagen plays an essential role in nucleation for mineralization.

### **1.4 NON-COLLAGENOUS PROTEINS**

Up to this point little is known about how mineralization is initiated and regulated. However, several macromolecules (Table 1) in the extracellular matrix are known to play a major role in

the initialization and regulation of mineral deposit. These macromolecules such as Osteonectin[7], Osteopontin[8], Dentin matrix protein 1[9], and Phosphophoryn[10] control the nucleation and crystal growth. These proteins are extremely negatively charged, rich in aspartic and glutamic acids, and serines which are often phosphorylated. The most studied family of non-collagen proteins is the SIBLING protein family[11] .

**Table 1** Major non-collagenous proteins in bone and dentin

Proteins originating in bone	Proteins originating in dentin
Bone Acidic Glycoprotein 75 (Bag 75)	Dentin matrix protein 1 (DMP1)
Bone Sialoprotein (BSP)	Dentin sialophosphoprotein (Dentin matrix DSPP)
Osteopontin (OPN, SPPI, 2ar, uropontin, Eta-1, 44 kDa phosphoprotein, 66 kDa phosphoprotein, 69 kDa phosphoprotein [pp69])	Dentin proteoglycans (D-PG I, D-PG II)
Osteonectin (SPARC, ON)	Matrix Gla Protein (MGP)
Bone Gla Protein (BGP, Osteocalcin)	Bone Gla Protein (BGP, Osteocalcin)
Matrix Gla Protein (MGP)	Osteopontin (OPN)
Decorin (PG II)	Osteonectin (SPARC, ON)
Biglycan (PG I)	
DMP1	
DSPP (low levels)	

## 1.5 SIBLING PROTEINS

A family of non-collagenous proteins contains an RGD motif which can interact with cell-surface integrins, and is termed Small Integrin-Binding Ligand, N-linked Glycoprotein (SIBLING). The proteins that belong to the SIBLING family are: osteopontin (OPN), bone sialoprotein (BSP), dentin matrix protein 1 (DMP1), dentin sialophosphoprotein (DSPP) which gives rise to dentin phosphophoryn (DPP) and dentin sialoprotein (DSP), and matrix extracellular phosphoglycoprotein (MEPE) [12]. These proteins, expressed in both bone and dentin, are secreted into the extracellular matrix during bone/dentin's formation and play a role in matrix mineralization. They interact with integrin receptors and mediate cell attachment and signaling. Their genes all are located in human chromosome 4q 21-23.

SIBLINGs are usually post-translationally modified by phosphorylation, glycosylation, sulphation, and proteolytic processing. Such post-translational modifications and the high levels of anionic amino acids make these proteins highly negatively charged; they can bind  $\text{Ca}^{2+}$  in solution or calcium hydroxyapatite[13], and were shown to have the ability to specifically bind collagen fibrils[14, 15]. Thus, these proteins may act as a linkage between the collagen fibril and mineral crystal. Some studies suggest that SIBLINGs undergo conformational changes from random coil to beta-pleated sheet and beta-turns in the presence of calcium [16, 17] .

**Table 2** Post-translational modifications of Sibling Proteins [18]

	Phosphate (Pi/mol)	CHO contents	N-Gly	O-Gly	SA	TGCH	Sulphation
OPN	13	16.6%	detected	detected	7.3%	detected	detected
BSP	5.85	50%	detected	detected	12%	detected	detected
DSP	6	29.5%	detected	detected	9%	unknown	unknown
HMW-DSP	10	detected	detected	detected	detected	unknown	unknown
DPP	209	unknown	unknown	unknown	unknown	unknown	unknown
DMP1-37K	12	unknown	unknown	unknown	unknown	unknown	unknown
DMP1-57K	41	unknown	unknown	unknown	unknown	unknown	unknown

### 1.5.1 Dentin Phosphophoryn (DPP)

The most abundant (>60% weight) non-collagenous protein produced by odontoblasts is dentin phosphophoryn. Dentin sialophosphoprotein (DSPP) is a precursor protein and has been never isolated from dentin extract. It is rapidly proteolytically processed to 3 proteins right after synthesis: dentin sialoprotein (DSP), dentin glycoprotein (DGP) and dentin phosphophoryn (DPP) which is rich in DSS repeat units, possibly by MMP-2 and MMP-20 [19]. (Figure 2)



DPP)[20]. DPP has the highest affinity for  $\text{Ca}^{2+}$  among all the matrix proteins studied. DPP was shown to bind to the collagen fibrils at the mineralization front while binding to calcium[15]. Thus, the phosphate groups on DPP may play an essential role in mineralization formation by providing the interface linkage of collagen and crystals.

### **1.5.2 Dentin Matrix Protein 1 (DMP1)**

DMP1 is another acidic extracellular matrix protein containing 64 aspartic acid, 77 glutamic acid and 115 serines out of total 503 amino acids. In comparison to DPP, DMP1 has a PI of 3.9. Sequence analysis shows that about 66 serines could be phosphorylated by casein kinase II and 29 serines could be phosphorylated by casein kinase I. DMP1 gene is also located on 4q21. Unlike DPP, DMP1 is found in both mineralizing (dentin, skeleton)[8] and non-mineralizing tissues (brain, kidney and salivary gland)[21].

DMP1 is required for both odontogenesis and osteogenesis (Figure 4). DMP1 was firstly shown to participate in biomineralization in MC3T3 cells, overexpression of DMP1 accelerated cell differentiation to odontoblast and initiated mineralization[22]. DMP1 was also found closely associated with the formation of bone nodule[23]. In proliferating preosteoblasts, DMP1 is predominately unphosphorylated in the nucleus [9]. During osteoblast maturation it becomes phosphorylated, and then secreted to the cytosol and extracellular matrix, where it orchestrates mineralization. This phosphorylation is believed to be catalyzed by a nuclear isoform of Casein Kinase II when  $\text{Ca}^{2+}$  surges into the nucleus [9]. Thus phosphorylation seems to play an essential regulatory role in DMP1 function. Besides mineralization regulator, DMP1 also act as a transcription regulator that initiates osteoblast differentiation [9].

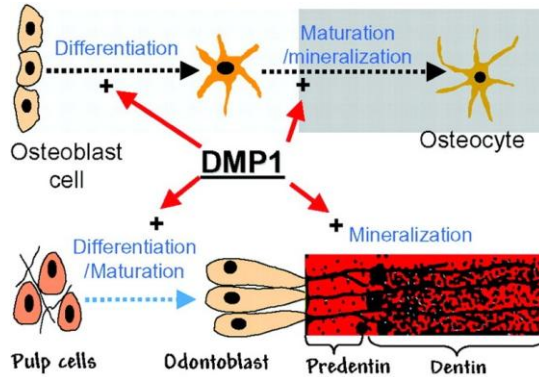


**Figure 4** DMP1 is required for both osteogenesis and odontogenesis

DMP1 is required for both osteogenesis and odontogenesis by controlling cell differentiation and maturation, as well as mineralization. Schematic from Qin et al. [24]

Similar to DSPP, full length DMP1 is cleaved to 2 functional fragments: 37kDa and 57kDa (Figure 5, 6). The uniformity cleavages at X-Asp bonds suggest a single responsible proteinase or a single proteinase group, which is still not known. Possible candidate include PHEX (phosphate-regulating gene with homologies to endopeptidases on X chromosome) proteinase [25], and BMP-1 (bone morphogenetic protein 1)/tolloid-like metalloproteinases [24]. These enzyme(s) are widely expressed and are not tissue specific.

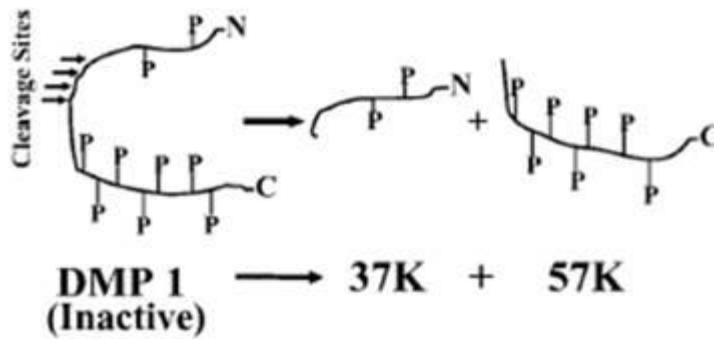


**Figure 5** DMP1 is cleaved into 2 fragments

Full length DMP1 is cleaved at X-Asp bonds to 2 functional fragments: 37kDa (N-terminal) and 57kDa (C-terminal) fragments

**MKTVILLVFLWGLSCALPVARYHNTESESSEERTGDLAGSPPPP  
 TNSESSEESQASPEGQANS DHTDSSSESGEELGYDRGQYRPAG  
 GLSKSTGTGADKEDDEDDSGDDTFGDEDNDLGPEEGQWGGPS  
 KLDSDEDSTDTTQSSDSTSQENSAQDTPSDSKDH DSEDEADS  
 RPEAGDSTQDSESEEQRVGGGSEGES SHGDGSEFDDEGMQSD  
 DPESTRSDRGHARMSSAGIRSEESKGDREPTSTQDSDDSQSVE  
 FSSRKSFR RSHVSEEDYRGELTDSNSRETQSDSTEDTASKEES  
 RSEQEDTAESQSQEDSPEGQDPSSSESSEEAGEPSQESSSESQ  
 EGV TSESRGDNPDNTSQAGDQEDSESSEEDSLNTFSSSESQST  
 EEQADSESNESLSLSEESQESAQDGDSSSQEGLQSQSASTESR  
 SQESQSEQDSRSEEDSDS QDSSRSKEESNSTGSASSSEEDIRP  
 KNMEADSRKLIVDAYHNKPIGDQDDNDCQDGY**



**Figure 6** Scheme of different forms of DMP1

Total AA: 503. Signal peptide: 1-16aa. The whole sequence is called full DMP1; the c-terminal part with signal peptide is c-DMP1. Signal peptide is required for *in vivo* study.



## 1.6 PHOSPHORYLATION BY EUKARYOTIC PROTEIN KINASES

The phosphorylation of critical seryl and threonyl by specific kinases is one of the most important post-translational modifications of SIBLING proteins. One of the largest groups of kinases is the eukaryotic protein kinases, which comprise a large superfamily of homologous proteins. They can transfer the gamma phosphate from ATP or GTP to the acceptor hydroxyl residue to generate phosphate monoesters. Based on the type of acceptor, there are two subfamilies: the protein-serine/threonine kinases which utilize aliphatic hydroxyl groups on serine and threonine; and the protein-tyrosine kinases which utilize the phenolic hydroxyl groups on tyrosine. Although there is a high diversity of structures and substrate specificities among different kinases, they all have catalytic domains which consist of approximately 250-300 amino acids, folding into a common catalytic core structure.

Among these eukaryotic protein kinases superfamily, casein Kinase I & II are messenger-independent protein kinases. They are defined by the fact they can phosphorylate acidic sequences such as in casein. Their activities are not depending on any known second messengers.

Casein Kinase I (CKI) is a monomer with a molecular weight of 30kDa. For CKI phosphorylation, the most effective recognition motif is pSXXS/T where there is a Ser containing phosphate groups in the position -3 [26]. Also, if there are clusters of acidic residues at the position -3, D/EXXS/T phosphorylation can also occur. The preference of phospho-serine leads to so called hierarchical phosphorylation. Especially, in a SXXS sequence, the phosphorylation of first Serine helps the second Ser to be phosphorylated by CKI[27].

Casein Kinase II (CKII) is a tetramer with an  $\alpha\alpha'\beta_2$  or  $\alpha_2\beta_2$  form. The molecular weight is 41kDa to 44kDa for  $\alpha$  subunit, 37kDa to 42kDa for  $\alpha'$  subunit, and 24kDa to 26kDa for  $\beta$  subunit[27]. The  $\alpha$  and  $\alpha'$  subunits are catalytic subunits, the  $\beta$  subunit is the regulatory subunit

with a potential metal-binding motif and can undergo N-terminal autophosphorylation. CKII can phosphorylate serine and threonine when there is a cluster of acidic amino acids or phosphoserine at position +3, **S/TXXD/E** or **S/TXXpS**[27]. As CKI, CKII also participates in hierarchal phosphorylation schemes.

## 2.0 HYPOTHESIS

Non-collagenous proteins (NCP) of bone/dentin are rich in phospho-proteins that do appear to play a major role in initiation and regulation of the mineralization process. These phospho-proteins possess a sequence rich in D and S which has the potential to be phosphorylated. Attention has been focused on studying the role of these proteins in mineralization, but the role of phosphorylation of these proteins and corresponding effects in mineralization is not understood.

**The goal** of this research is to elucidate the mechanisms involved in phosphorylating the highly phosphorylated proteins of bone and dentin, Emphasis will be placed to phosphorylation of DPP and DMP1 since they are the most phosphorylated proteins in the bone/dentin extracellular matrix. These data will be critical to prove **the general hypothesis** of our research that the phosphorylation level of non-collagenous proteins play a significant role in matrix-mediated mineralization.

## **3.0 MATERIAL AND METHODS**

### **3.1 REAGENTS AND MATERIALS**

[ $\gamma$ -<sup>32</sup>P] ATP of specific activity was purchased from ICN Biomedical Inc. Reagents for SDS-polyacrylamide gel electrophoresis was obtained from Bio-Rad. Casein Kinases' assay kit was obtained from Millipore. All other chemicals for phosphorylation assays, subcellular fractions and zymogram were purchased from Sigma. All medium for cell culturing are from GIBCO.

### **3.2 RECOMBINANT PROTEIN PURIFICATION**

#### **3.2.1 Constructs and mutation**

Several forms of DPP were used for in vitro phosphorylation as shown in figure 3,

- Original recombinant PP (rPP) plasmid PGEX-4T-3-pp was cloned by Dr. Sfeir. This clone was designed to include the [DSS] repeats, but it lacked the N-terminal end of the protein.
- C-stop rPP is made by inserting a stop codon to PGEX-4T-3-pp using Quikchange XL site-Directed Mutagenesis Kit (STRATAGENE Catalog # 200517) using the following

primers: Primer 1 (5' gttctgacagcagt tag ggtgacagcaagtctg 3') and primer 2 (5' cagacttgctgcacc cta actgctgtcagaac 3') (Table 3).

**Table 3** Cycles of PCR

Segment	Temperature	Time	cycles
1	95°C	1 minute	1
2	95°C	50 seconds	18
	60°C	50 seconds	
	68°C	8 minutes (1 min / Kb of plamid)	
3	68°C	7minutes	1
4°C			

- Full length DPP (fPP) was generating by cloning the full length of exon 5 which includes the N-terminal end. (Figure 3).C-stop fPP is made using the same methods as C-stop rPP

The C-terminal and full length DMP1 clones were obtained from Dr. Jian Feng's Laboratory at Baylor school of Dental Medicine.

All mutations (Figure 3) were confirmed by Sequencing in Proteomics & Genomics Core Lab, University of Pittsburgh.

### **3.2.2 Recombinant protein purification**

All clones were transformed into BL21 bacteria, and were cultured in autoclaved Luria Broth with 50ug/ml ampicillin, 37°C. Protein expression was induced by adding 0.1mM IPTG to cultured BL21 with an OD 0.8, then culture for another 4 hours. After 10,000 RPM centrifugation for 45min at 4°C in JA-12 rotor, bacteria (pellets) were collected and sonicated, treated with 1% Triton X-100, 0.06% beta-mercaptoethanol and 10mM MgCl<sub>2</sub>. GST sepharose 4B beads. GST-tag protein was eluted in 10mM Glutathione, 1M Tris pH8.0 or further cleaved by biotinylated-thrombin.

Purified proteins were dialyzed in ddH<sub>2</sub>O using Amicon Ultra-15 Ultracel-10K (Millipore) and centrifuged at 5000g, 30min, 3 times. Protein concentrations were measured using a BCA kit.

### **3.3 TISSUE CLUTURE OF CELLS**

MC3T3 were cultured in Minimum Essential Medium-alpha Medium. MDPC23 were cultured in alpha-modified medium. NIH3T3, Hela, 293 were cultured in DMEM. All media were supplemented with 10% fetal bovine serum, 10% L-Glutamine and 10% Penicillin-streptomycin.

### 3.4 DMP1 PURIFICATION FROM CELLS

Cells were grown to 80% confluence in normal media, then serum free media was used, and 10ul of adenovirus-CMV-DMP1 ( $2 \times 10^{12}$  pt/ml) per 150mm plate was added. The cells were maintained in culture for 48 to 96 hours, the cell media was collected, concentrated and buffer exchanged in 6M urea in 20mM Tris-HCl, using Amicon Ultra-15 Ultracel-10K (Millipore). Cells were trypsinized with 0.05% trypsin, 0.53mM EDTA (Gibco-BRL), then washed and collected in lysis buffer containing phosphatase inhibitor cocktail (50mM  $\text{NH}_4\text{HCO}_3$ , 5mM TCEP, 1mM EDTA, 1mM PMSF and protease inhibitor cocktail (5mM Sodium Orthovanadate, 10mM NAF, 25mM beta-Glycerophosphate). Homogenization was carried out on ice in a glass homogenizer at low speed 333 rpm (Glas-Col, LLC) for about 30 strokes. The cell lysate was then subjected to a exchange buffer to 6M urea in 20mM Tris-HCl.

The cell media or cell lysate in 6M urea, 20mM Tris-HCl were loaded onto ion-exchange column (HiTrap™ Q FF 5ml column from GE Healthcare) using an FPLC(AKTA primer plus from GE Healthcare). The gradient used to elute the proteins was 0.1M NaCl (Buffer A) to 1M NaCl (Buffer B) in 80min. Fractions corresponding to each peak were collected and analyzed by SDS-PAGE and stains-all stain.

Buffer A: 6MUrea in 20mM Tris-HCl+0.1M NaCl (pH=7.2)

Buffer B: 6MUrea in 20mM Tris-HCl+1M NaCl (pH=7.2)

### **3.5 CELL CYTOSOLIC AND MEMBRANOUS FRACTIONS PREPARATION**

The MC3T3 /MDPC23 cells were collected ( $4 \times 10^6$  cells/flask), trypsinized with 0.05% trypsin, 0.53mM EDTA(Gibco-BRL), washed and homogenized in a solution of 50mM Tris-Hepes pH7.4, 1mM EDTA, 10mM Manitol, 1mM Dithiothreitol, 1 pill of Complete Protease inhibitor cocktail tablets(Roche Applied Science). Homogenization was carried out on ice in a glass homogenizer at low speed 333 rpm (Glas-Col, LLC) for about 30 strokes. The homogenate were centrifuged at 1,000g for 20min to sediment the nuclei and cell debris. The low speed pellet (nuclei and cell debris) and supernatant were collected separately. The supernatant was further centrifuged at 100,000g for 30min to obtain the cytosolic and membranous fractions. All these fractions were stored at  $-80^{\circ}\text{C}$  and thawed before their use for zymogram analysis or in vitro phosphorylation assays. Figure 7 shows the cell fractionation scheme. We used supernant 2 for zymogram analysis and used pellet 1, pellet 2 and supernant 2 for in vitro phosphorylation assays.



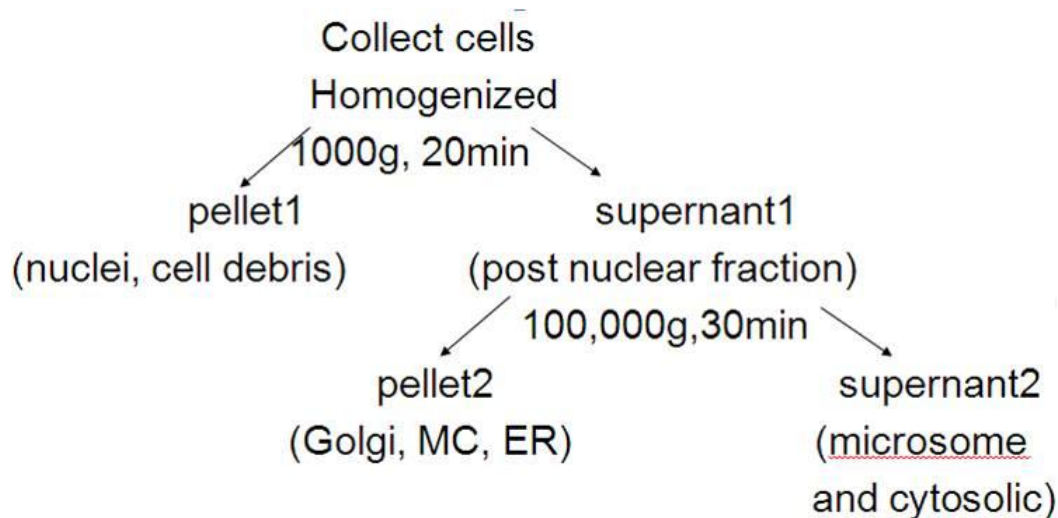


**Figure 7** Strategy for subcellular fraction

The cells were collected and homogenized and centrifuged. The low speed pellet (nuclei and cell debris) and supernatant were collected separately. The supernatant was further centrifuged at 100,000g for 30min to obtain the cytosolic and membranous fractions.

### 3.6 *IN VITRO* PHOSPHORYLATION

#### 3.6.1 *In vitro* phosphorylation by CKI and CKII

The *in vitro* phosphorylation reaction was carried out in 40ul total volume, containing 10ul assay dilution buffer I (20mM MOPS, pH7.2, 25mM beta-glycerol phosphate, 5mM EGTA, 1mM sodium orthovanadate, 1mM dithiothreitol), 100ng Casein Kinase I or Casein Kinase II, dialysed protein substrate, ddH<sub>2</sub>O, 10ul 1μCi/μl Mg/ATP and [γ-<sup>32</sup>P] mixture. The reaction solution was incubated for a range of time (30min to overnight) in a shaker incubator at 30°C or 37°C. The controls consisted of carrying out the phosphorylation reaction with the enzyme only

(sample with enzyme but no protein substrate) and a protein only control (sample with protein substrate but no enzyme).

### **3.6.2 *In vitro* phosphorylation by cell fractions**

Cell fractions were prepared as described in section 3.5. Insoluble fractions such as pellet 1, pellet 2 were treated with Triton X-100 at 4°C for 1hour, then the sample was centrifuged at 1000g for 5min and then the supernatant was collected. The soluble fractions were added to the reaction solution directly. Each reaction tube contains 10ul ADBI buffer (Assay Dilution Buffer I as suggested by company), cell fractions, 10μl 1μCi/μl Mg/ATP and [ $\gamma$ -<sup>32</sup>P] mixture. The reaction solution was incubated for a range of time (30min to overnight) in a shaker incubator for 30°C or 37°C.

### **3.6.3 Phosphorylation quantification by scintillation counter**

#### **3.6.3.1 Measurement on P81 paper square**

Upon completion of the phosphorylation reaction, 25 μl were transferred onto the center of a 2cmx2cm P81 paper square. The radiolabeled solution was allowed to bind to the filter paper. The P81 paper square was washed 3 times with 40ml 0.75% phosphoric acid in a 50ml conical tube. The P81 paper was gently shaken for 5 minutes per wash on a rotator. Then the P81 paper was washed with 20ml acetone and shaken for 5 minutes. All washes were discarded in a liquid radioisotope waste container. The P81 paper square was then allowed to drain for 5 min and then transferred to a scintillation vial where 5ml scintillation cocktail was added and the radioactivity was quantified using a scintillation counter.

### **3.6.3.2 Measurement using centrifugal filter devices**

Upon completion of the phosphorylation reaction, the total volume was transferred to a 10kD microcon centrifugal filter devices (Millipore), ddH<sub>2</sub>O was added to a final volume of 200μl, then centrifuged at 14,000xg for 30min. The filter was washed again in 200μl ddH<sub>2</sub>O, centrifuged at 14,000 x g for another 30min. The filter device was removed from the eppendorf tube and placed directly into the scintillation vial. 5ml scintillation cocktail was added, and radioactivity was quantified in a scintillation counter.

### **3.6.4 Phosphorylation detection by SDS-Gel**

Upon completion of the phosphorylation reaction, 8 μl of 6x Loading buffer (0.35M Tris-HCl PH6.8, 10.28% SDS, 36% glycerol, 0.6 MDTT, 0.012% Bromophenol blue) was added to the each 40 μl reaction sample and then boiled for 5min at 95°C. The samples were loaded on an 8% SDS-PAGE and run for 2hour at 100V. The gel was then dried on filter paper (Bio-rad) using Model 583 Gel Dryer (Bio-Rad) and exposed to Kodak X-Omat Blue XB-1 film to detect labeled bands.

## 3.7 MASS SPECTROMETRY

### 3.7.1 In gel digestion

Typically, samples were run in an 8% SDS-gel at 90V for 30 minutes and then 120V for 90 minutes. Following the staining and destaining procedures, gel bands of interest were excised and collected pieces in a 600  $\mu$ l tube. 100  $\mu$ l of 50% Acetonitrile, 50mM Ammonium bicarbonate were added, we made sure the gel were well soaked, shook at room temperature for 30 minutes, the washing step was repeated twice. Finally, we added 50  $\mu$ l of 100% Acetonitrile, then shook the sample for 5min, and dry the gel in Speed Vac.

The dried gel pieces were reduced in 100  $\mu$ l of 2mM Tris (2-carboxyethyl) phosphine (TCEP), 25mM Ammonium biocarbonate (pH 8.0), and incubated for 15 minutes at 37°C. The gel pieces were then alkylated in 100  $\mu$ L of 20 mM iodoacetamide, 25 mM ammonium bicarbonate (pH 8.0) and incubate for 30 minutes at 37°C in the dark. After reduction and alkylation, the supernatant was discarded, the gel band was washed three times with 200  $\mu$ L of 25 mM ammonium bicarbonate, and each time the sample was shaken for 30 minutes. Then 50  $\mu$ L of acetonitrile was added, shaken for 5 minutes and dried in a Speed Vac.

The gel slice was digested with trypsin. To allow the concentrated trypsin to diffuse into the gel slice, the gel was rehydrated in 10  $\mu$ l from a stock solution of 0.02  $\mu$ g/ $\mu$ l of Promega Sequencing grade modified trypsin in 10% Acetonitril, 40 mM  $\text{NH}_4\text{HCO}_3$  pH 8 for 1 h on ice. The excess of trypsin that hasn't been absorbed into the gel slice was removed, the gel slice was then covered with 50  $\mu$ l of 10% Acetonitril, 40 mM  $\text{NH}_4\text{HCO}_3$  pH 8.0, and was placed in a shaker incubator at 37°C overnight.

The peptides generated from the trypsin digestion were extracted by transferring the supernatant to a fresh tube, adding 50µl of 50% Acetonitril, 5% Formic acid to gel slice and shaking the samples for 30minutes at 37°C. This step was repeated twice to extract more digested material. The extracted samples were then dried in Speed Vac, then resuspended in 200 µl H<sub>2</sub>O, to be dried a second time in the Speedvac to remove all ammonium bicarbonate and Acetonitrile. The digestion was finally cleaned by ziptipC18 if necessary.

### **3.7.2 In solution digestion**

Protein samples were desalted using desalting column (Pierce), concentrated using a speedvac, add 25 mM ammonium bicarbonate to 40µl, sample is reduced by adding 1.2 µl of 100 mM TCEP (tris-2-carboxyethyl-phosphine) to 5mM final, shake for 15 minutes at 37°C. 0.88 µl of 500 mM IAA (Iodoacetamide) was added to 10 mM final concentration and was shaken in the dark for 30 minutes. The remaining IAA was neutralized by adding 20 ul of TCEP stock, vortexed, spun, and incubated at room temp for 45 min. Then added trypsin to sample ratio should be between 1:50 to 1:20. Digestion was allowed to incubate at 37°C overnight. Digestion was acidified by adding formic acid to stop the reaction and then dried in Speed Vac and cleaned by ziptipC18 if necessary.

### **3.7.3 MALDI-TOF MS**

For MALDI-TOF-MS analysis, the peptides and CHCA matrix ( $\alpha$ -Cyano-4-hydroxycinnamic acid, about 10 µg/ µl, in 50%ACN and 0.1% TFA) solutions were premixed in a small Eppendorf tube, spun down and mixed 3 times, and applied directly to the sample plate. Once the

sample is applied to the sample support, the sample was allowed to air dry. Other matrix such as Trihydroxyacetophenone (THAP), 3, 5-Dimethoxy-4-hydroxycinnamic acid (sinapinic acid) prepared according to Voyager instruction were also used in this study. The samples were all analyzed using the Voyager DE Pro (ABI) or 4700 TOF TOF (ABI) instruments.

#### **3.7.4 LC-ESI MS**

For LC-ESI MS analysis, samples were dissolved in 0.1% formic acid, run through a C18 column. The buffer A contained 0.1% formic acid in water while buffer B contains 0.1% formic acid in acetonitrile. Experiments were conducted on LCQ-DECA-XP (ThermoFinnigan) and LTQ-XL (ThermoElectron) instruments.

### **3.8 ZYMOGRAM**

#### **3.8.1 Detection of the kinase activity after 1-Dimension SDS-PAGE**

The cell fractions were prepared as described in section 2.5, and mixed with 6X loading buffer (0.35M Tris-HCl PH6.8, 10.28% SDS, 36% glycerol, 0.6 MDTT, 0.012% Bromophenol blue). The mixture was electrophoresed on an 8% SDS-pollyacrylamide gel containing 60 µg/ml of DMP1. The DMP1 protein was added to the SDS-PAGE prior to polymerization. Following the sample electrophoresis at 100V for 2 hours in an 8x8 cm gel, the SDS was removed first by washing the gel in 100 ml 20% iso-propanol in 50mM Tris-HCl, pH8.0 for 1 hour, this step was repeated once. Then the gel was washed with 250ml of 50mM Tris-HCl, pH 8.0 containing 5mM

2-beta mercaptoethanol for 1 hour at room temperature. The enzyme within the gel was denatured by treating the gel with 100ml 6M HCl-Guanidine for 1 hour at room temperature, and this denaturing wash was repeated a second time. Following the denaturation of the enzyme, the enzyme was renatured by five washes of 250ml 50mM Tris-HCl, pH 8.0 containing 5mM 2-β mercaptoethanol and 0.04% Tween 40 at 4°C for total 16 hours.

To detect the enzyme activity in the cell fractions, the gel was incubated overnight in 60ml phosphate buffer solution, which contains 50mM Tris-HCl, pH7.4, 5mM MgCl, 10mM beta-glycerophosphate, 50μM ATP and 300μCi [ $\gamma$ -<sup>32</sup>P] ATP.

After incubation, the gel was washed in a buffer containing 5% trichloroacetic acid solution and 1% sodium pyrophosphate 7 times, until the radioactivity of the solution became negligible. The gel was then dried on filter paper (Bio-Rad) using Model 583 Gel Dryer (Bio-Rad) and exposed to Kodak X-Omat Blue XB-1 film to detect labeled bands. Usually 3 hours or longer (overnight) exposure was required for detection.

### **3.8.2 Kinase identification using mass spectrometry**

The radioactive gel was stored in -80°C for one month for the radioactivity to decay. The gel bands corresponding to labeled bands were excised, and then treated as described in section 2.7.1.

## **4.0 RESULTS AND DISCUSSION**

In order to study the level of phosphorylation of PP and DMP1, we generated different forms (Figure 3, Figure 6) of these two proteins as described in section 3.2.

Full length DPP (fPP)

Recombinant PP (rPP): the N-terminal sequence was deleted from the fPP. This protein is primarily made of the [DSS] repeats

C-stop PP (cPP): the C-terminal sequence was deleted from rPP by inserting a stop codon following the DSS repeat sequence.

In regards to DMP1, we studied the two different forms of DMP1 based on the identified cleavage site. [23]. The full length DMP1 is called fDMP1, and the c-terminal region with signal peptide is called cDMP1 which is where the phosphorylation sites are located.

### **4.1 MASS SPECTROMETRY OF PP**

In order to study the phosphorylation of PP by mass spectrometry, we digested the unphosphorylated rPP first. For rPP, which has extensive DSS repeat, we used EXPASY to identify the enzyme lists which might be able to cleave rPP. (Table 4)



**Table 4** List of enzymes and chemicals that might cleave rPP

Enzymes can cleave rPP	#. of Cleavages	Positions	Cleavage sites
Arg-C proteinase	1	5	Arg-C
Chymotrypsin			Y, F, W (preferred) /L, M, H/A, D, E -C
Clostripain	1	5	Arg-C
Asp-N endopeptidase	ALL D		N - Asp
Lys-N/Lys-C	4	53 70 415 427/5 4 71 416 428	N-Lys/Lys-C
Proteinase K	7	8 10 11 26 132 250 457	Y, F, W-C
Hydroxylamine	2	44 431	Asn-Gly
Trypsin	4	5 71 416 428	K,R-C
Endo Glu-c	9	1 14 28 50 52 56 69 283 449	Glu-C
NTCB (2-nitro-5-thiocyanobenzoic acid)	2	132 179	N-Cys
Thermolysin	2	25 249	N-A,I,L,V,M,F D,E-Xcan't be cleaved
Formic acid	ALL D		D-C (preferred) /N-D

Based on the data shown in Table 4, we concluded that PP would be hard to digest/cleave, the numbers of enzymes/chemicals that can cleave PP were limited, and most of them can only cut very few sites. We tried all enzymes and chemicals listed in this table except the ones that display only one cleavage site (Thermolysin, Arg-C proteinase, Clostripain, Hydroxylamine) , or LysN/C which would produce peptide either too small or too large for mass spectrometry analysis. Figure 8 shows the SDS gel of fPP after digestion by proteinase K, chymotrypsin, asp-N, Endo-GluC and Trypsin. The disappearance of protein band and appearance of some smaller bands suggest that the protein was digested. From this gel, we observed that AspN, proteinase K and formic acid (data not shown) completely cleaved fPP, while trypsin, chymotrypsin and endo-GluC cleaved fPP to a certain extent. fPP was not cleaved at all by NTCB(data not shown)

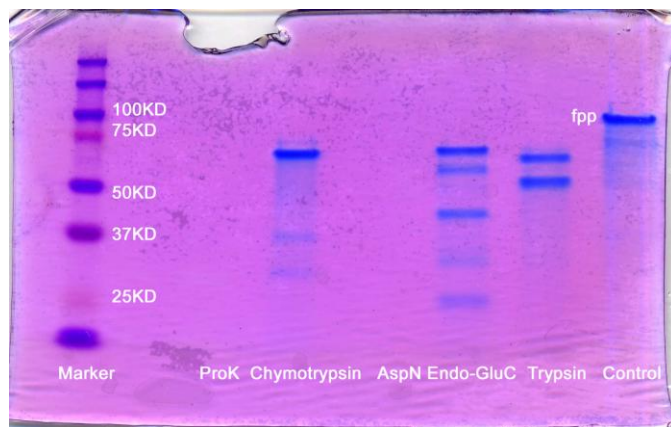


**Figure 8** fPP cleaved by enzymes and chemicals

AspN and proteinase K completely cleaved fPP, while trypsin, chymotrypsin and endo-GluC cleaved fPP to a certain extent.

Based on the SDS gel result, we digested rPP using trypsin, chymotrypsin, Endo-GluC separately or together. We also used asp-N, formic acid digestion at different time points, from 1 hour to 18 hour. The digested protein was then analyzed by mass spectrometry using different matrices such as CHCA, THAP and SA, however, we couldn't obtain any peptide signal from rPP. This might be due to the acidic nature of rPP which makes the peptide highly negative charged. Another possibility could be due to the improper peptide size following digestion, e.g, peptides produced by Asp-N are too small, and peptides produced by trypsin are too large.

## **4.2 MASS SPECTROMETRY OF DMP1**

cDMP1, which is less acidic than rPP and contains more amino acids other than "DSS" repeat, have been successfully digested and analyzed. Theoretically, the combination of 2 enzymes (Trypsin and AspN) can digest 95% of DMP1. Figure 9 and Figure 10 show cDMP1 digested by Trypsin/AspN and analyzed on ABI 4700 MALDI-TOF-MS. Peptides signal identified are labeled.

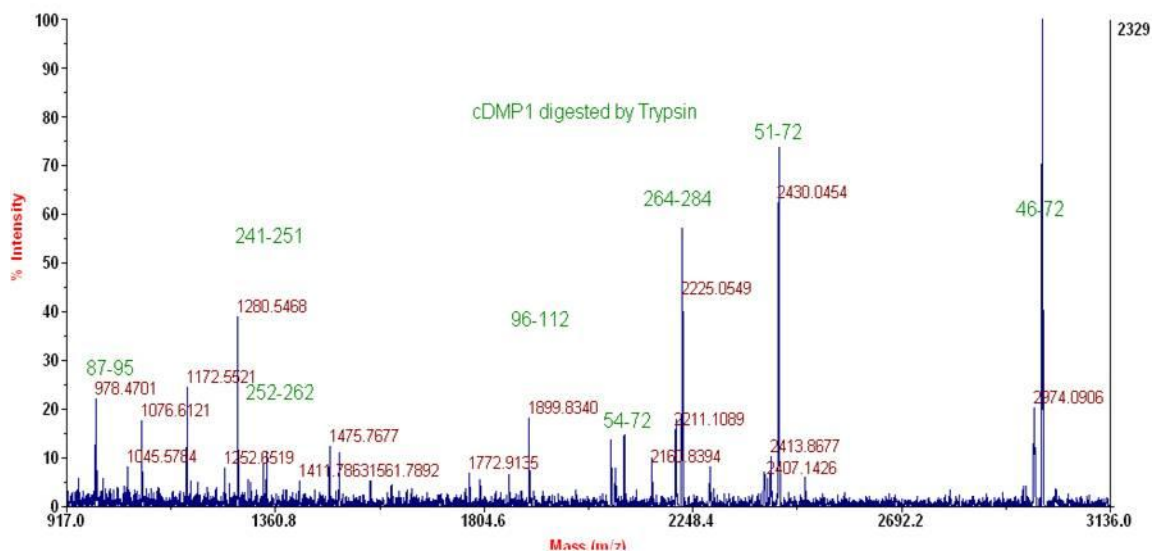


**Figure 9** cDMP1 digested by trypsin

Green labels represent numbers of DMP1 amino acids in identified fragments. Coverage: 31%

Identified peptide	Expected ms	Observed ms	Amino acid position
GELTDSNSR	978.4	978.4	87-95
SQESQSEQDSR	1280.5	1280.5	241-251
SEEDSDSQDSSR	1341.5	1341.6	252-263
ETQSDSTEDTASKEESR	1899.8	1899.8	96-112
EPTSTQSDSDSQSVEFSSR	2101.8	2101.8	54-72
SKEESNSTGSASSSEEDIRPK	2225.0	2225.1	264-284
GDREPTSTQSDSDSQSVEFSSR	2430.0	2430.0	51-72
SEESKGDREPTSTQSDSDSQSVEFSSR	2990.3	2990.1	46-72

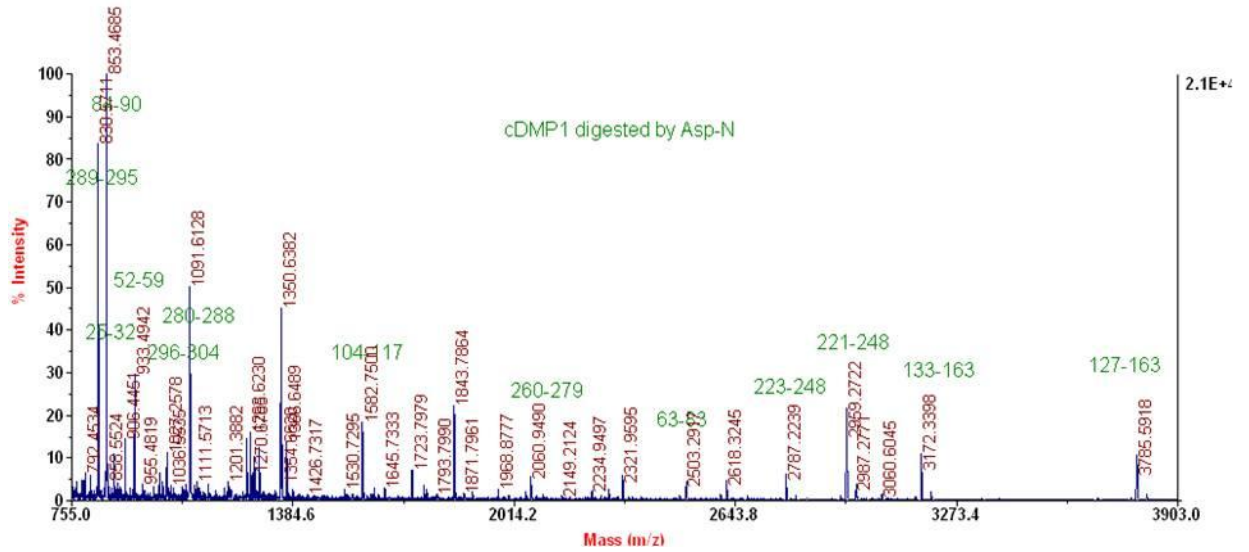


**Figure 10** cDMP1 digested by AspN

Green labels represent numbers of DMP1 amino acids in identified fragments. Coverage:48%

Identified peptide	Expected ms	Observed ms	Amino acid position
DSRKLIV	830.5	830.6	289-295
DYRGELT	853.4	853.5	84-90
DDPESTRS	906.4	906.4	25-32
DIRPKNMEA	1089.5	1089.6	280-288
DAYHNKPIG	1014.5	1014.5	296-304
DTASKEERSSESQE	1582.7	1582.8	104-117
DSSRSKEESNSTGSASSEE	2060.8	2060.9	260-279
DSQSVEFSSRKSFRSSHVSE E	2484.2	2483.0	63-83
DSSSQEGLQSQSASTESRSQ ESQSEQ	2787.2	2787.2	223-248
DGDSSSQEGLQSQSASTESRSQESQSEQ	2959.1	2959.3	221-248
DPSSSESSEEAGEPSQESSSESQEGVTSESRG	3172.3	3172.3	133-163
DSPEGQDPSSSESSEEAGEPSQESSSESQEGVTSESRG	3785.5	3785.6	127-163

### 4.3 IN VITRO PHOSPHORYLATION OF PP

When we performed the in vitro phosphorylation of PP by CKI, we determined that the phosphorylation level detected using the scintillation counter technique is very low, e.g, only about 4 phosphates per molecule. When we determined the in vitro phosphorylation of both cPP and fPP using the scintillation counter, we obtained much higher phosphorylation levels than rPP (Figure 11) However, when we loaded the radio-labeled proteins on an SDS-PAGE, fPP showed less phosphorylation level than rPP while cPP still has higher levels of phosphorylation. These results suggest that PP might be too acidic to bind the negative charged P81 paper, the reason why fPP has higher level might due to stronger binding ability to P81 paper. The low binding might also be the reason of low phosphorylation level detected using scintillation counter. The low binding scenario was confirmed when we synthesized peptides based on the PP sequence that we then phosphorylated in vitro. The acidic peptide with only DSS repeat couldn't be detected by scintillation counter, whereas, the phosphorylation of the modified peptide with a basic N-terminus could be detected and quantified.

Since using the scintillation counter method to quantify the level of phosphorylation did not seem to be adequate we then decided to use a Microcon centrifugal filter device instead. Following three washes of the sample, the excess  $^{32}\text{P}\gamma[\text{ATP}]$  could not be removed which yielded a very high background. So far to determine the phosphorylation of PP is still unresolved.

Although we couldn't quantify the total amount of phosphate or the number of phosphorylation sites using mass spectrometry, we used radioactive  $^{32}\text{P}\gamma[\text{ATP}]$  in combination with an SDS-PAGE to quantify the amount of phosphate using densitometry. The radioactive SDS-PAGE gel (Figure 12) shows that the cPP phosphorylation was enhanced compared to rPP

phosphorylation. Quantification by densitometry using Kodak 1D software (Figure 13) shows that the deletion of the c-terminus could enhance the phosphorylation level to about 1.5 times of rPP.

The phosphorylation reaction was carried out by different enzymes kinases (Figure 14) shows that CKI could phosphorylate rPP much more than CKII, although sequence analysis suggest CKII is preferred than CKI; the combination of CKI+CKII did not show much phosphorylation enhancement. We also tested different time scales to phosphorylate rPP by CKI (Figure 15), the data shows that the phosphorylation level increases with longer incubation time.

Based on these assay results, we used CKI to phosphorylate the c-stop PP and incubated it for 23 hour or longer to get higher phosphorylation levels in our related mineralization study.

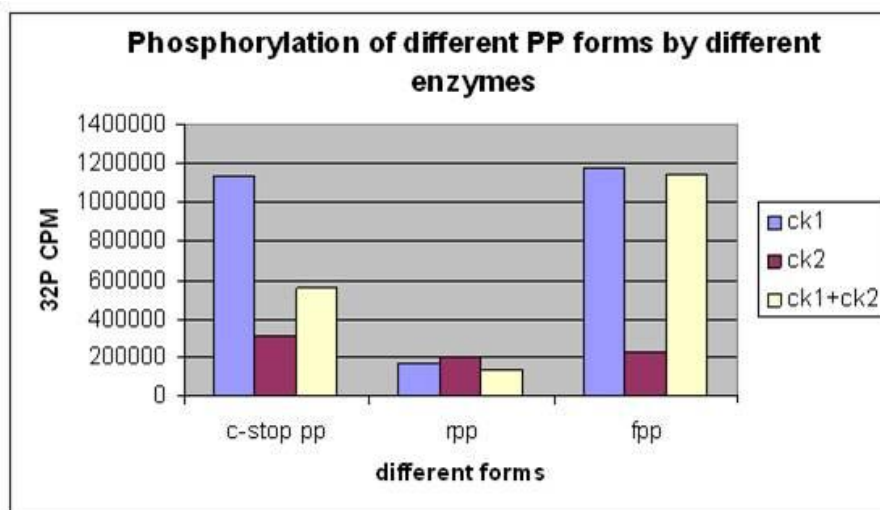


**Figure 11** Comparison of in vitro phosphorylation of different PP forms

Same mole amount rPP /fPP /c-stop PP are compared by scintillation counter. These differences might come from the different ability of different PP forms to bind to the P81 paper; it couldn't represent the different phosphorylation level. The comparisons by SDS-gel below are more accurate.

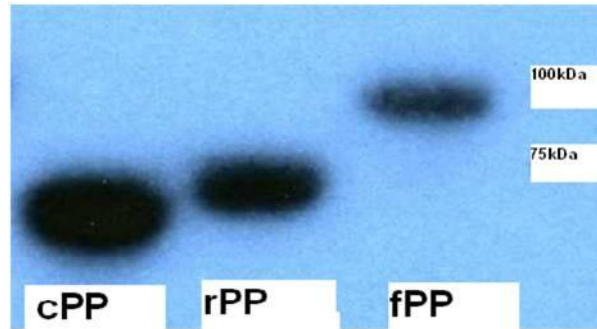


**Figure 12** In vitro phosphorylation of different PP forms by CKI

Same mole amount rPP /fPP /c-stop PP phosphorylation level are compared by radioactive SDS-Gel. This method of relative comparison of PP phosphorylation might be more accurate than the scintillation counter method. As the SDS-PAGE analysis circumvents the possible lack of PP binding to P81 paper needed for scintillation counter analysis. The phosphorylation level of cpp is higher compared to rpp and fpp. fpp is the lowest.

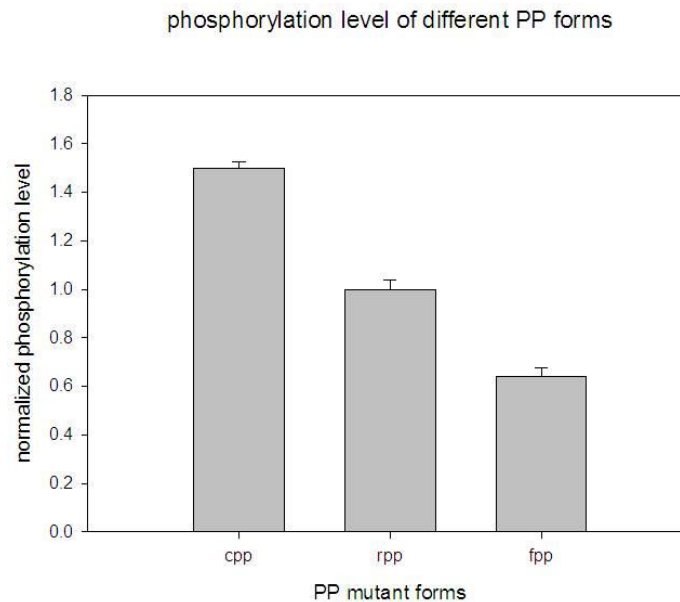


**Figure 13** Quantified comparison of in vitro phosphorylation of different PP forms by CKI

Same mole amount rPP /fPP /c-stop PP phosphorylation level are compared by radioactive SDS-Gel as in figure 12; these experiments are repeated 3 times and quantified by Kodak 1D software.



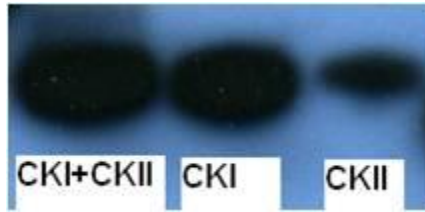


**Figure 14** Comparison of rPP phosphorylated by different enzymes

This data shows that CKI has the ability to phosphorylate rPP much more than CKII, although sequence analysis suggest CKII is preferred than CKI; the combination of CKI+CKII did not show a strong phosphorylation synergy between both enzymes.

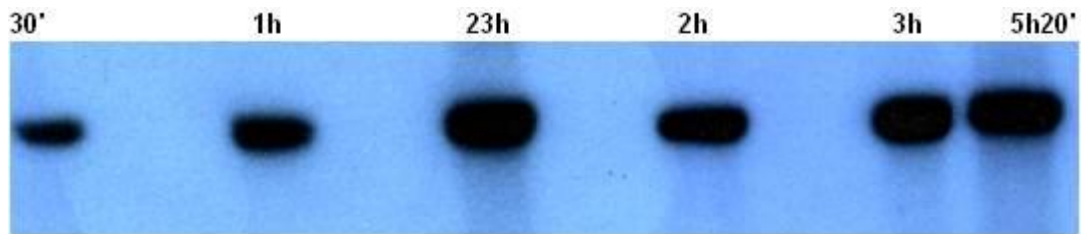


**Figure 15** In vitro phosphorylation of rPP by different time scale

In vitro phosphorylation of rPP by CKI yielded higher  $^{32}\text{P}$  incorporation onto rPP at longer incubation time when assessed by radiolabelled SDS-PAGE. Compared to 30min (normalized as 1), the phosphorylation level at 1h is 1.69, 2h is 1.82, 3h is 1.94, 23h is 2.05.

Since PP was proved difficult to analyze by mass spectrometry, we shifted our attention to DMP1 to study its phosphorylation and ultimately the effect of phosphorylation on mineralization.

#### 4.4 IN VITRO PHOSPHORYLATION OF DMP1

Our goal is to phosphorylate DMP1 and identify the phosphorylation sites in DMP1 with various levels of phosphorylation. We first study in vitro phosphorylation of fDMP1 and cDMP1 which both showed similar level of phosphorylation. We then decided to focus only cDMP1 phosphorylation since it contains most of the phosphorylation sites. To optimize the in vitro phosphorylation of cDMP1, we assessed the phosphorylation level by using different conditions including temperature, type of enzyme, time, and  $\text{Ca}^{2+}$  concentration.

The phosphorylation reaction was carried out at 30°C (the recommended temperature by the enzyme manufacturer) and 37°C (body temperature of mice). The level of phosphorylation of cDMP1 at 30°C and 37°C remains the same when assessed by scintillation counter (Figure 16).

The phosphorylation reaction was also carried out using different enzymes, although sequence analysis shows that CKII would phosphorylate more sites than CKI (Figure 17), our data shows that CKI phosphorylated cDMP1 about 5 folds more than CKII.

The phosphorylation reaction was carried out at different time scales; Figure 18 shows that the phosphorylation level of cDMP1 increases with longer incubation time.

The phosphorylation reaction was assessed at different calcium concentration, the increase of calcium, up to 2mM  $\text{Ca}^{++}$  seems to enhance the phosphorylation activity of CKI; if the calcium phosphorylation is >2mM then the phosphorylation activity was reduced as shown in Figure 19. This enhancement under 2mM of  $\text{Ca}^{++}$  might be due to the confirmation change of DMP1 and the formation of DMP1-Ca complex[16, 17]. However, when higher calcium concentration were used (>2mM), this might trigger DMP1 polymerization, which might explain the decrease in the ability of the kinase to phosphorylate the protein.

The phosphorylation reaction was also assessed at different magnesium concentration; the phosphorylation level increase between 1mM to 10mM, higher (>30mM) Mg<sup>++</sup> concentration inhibit the phosphorylation ability of the protein kinase, which might be due to the polymerization of the protein similar to the high Ca<sup>++</sup> concentration (Figure 19).

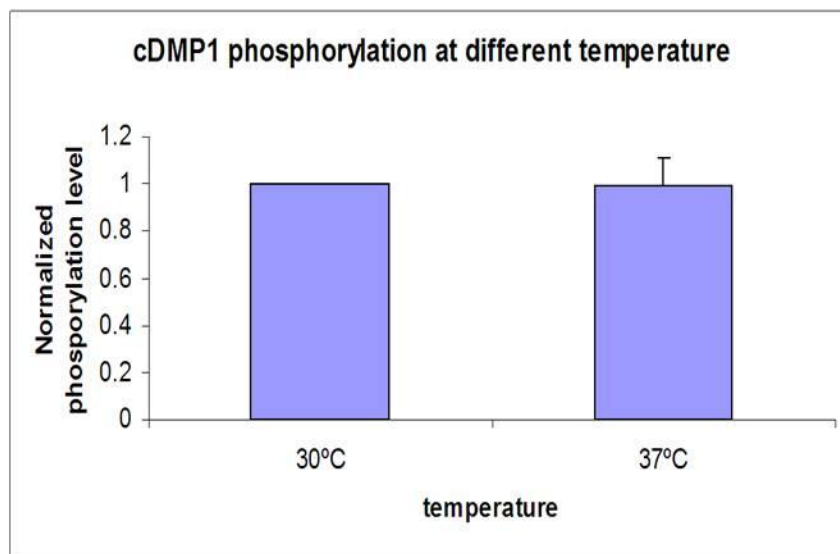


**Figure 16** In vitro phosphorylation of cDMP1 at different temperatures

The level of phosphorylation of cDMP1 at 30°C and 37°C (1 hour incubation) remains the same when assessed by scintillation counter

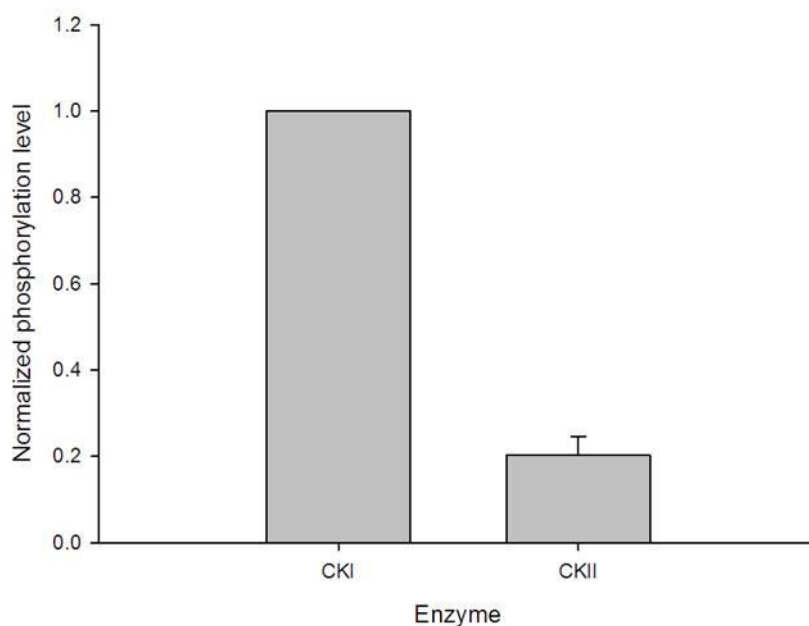


**Figure 17** In vitro phosphorylation of cDMP1 by CKI and CKII

CKI phosphorylated cDMP1 about 5 folds more than CKII when assessed by scintillation counter.

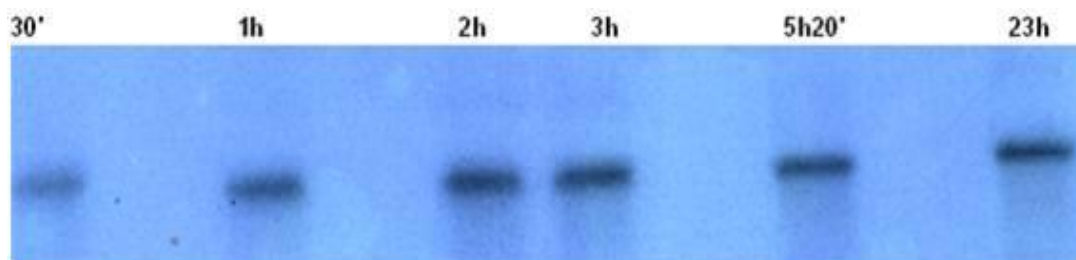


**Figure 18** In vitro phosphorylation of cDMP1 at different time points

In vitro phosphorylation of cDMP1 by CKI shows higher phosphorylation level with longer incubation time assessed by radiolabelled SDS-PAGE. Compared to 30min (normalized as 1), the phosphorylation level at 1h is 1.50, 2h is 1.51, 3h is 1.68, 23h is 1.85.

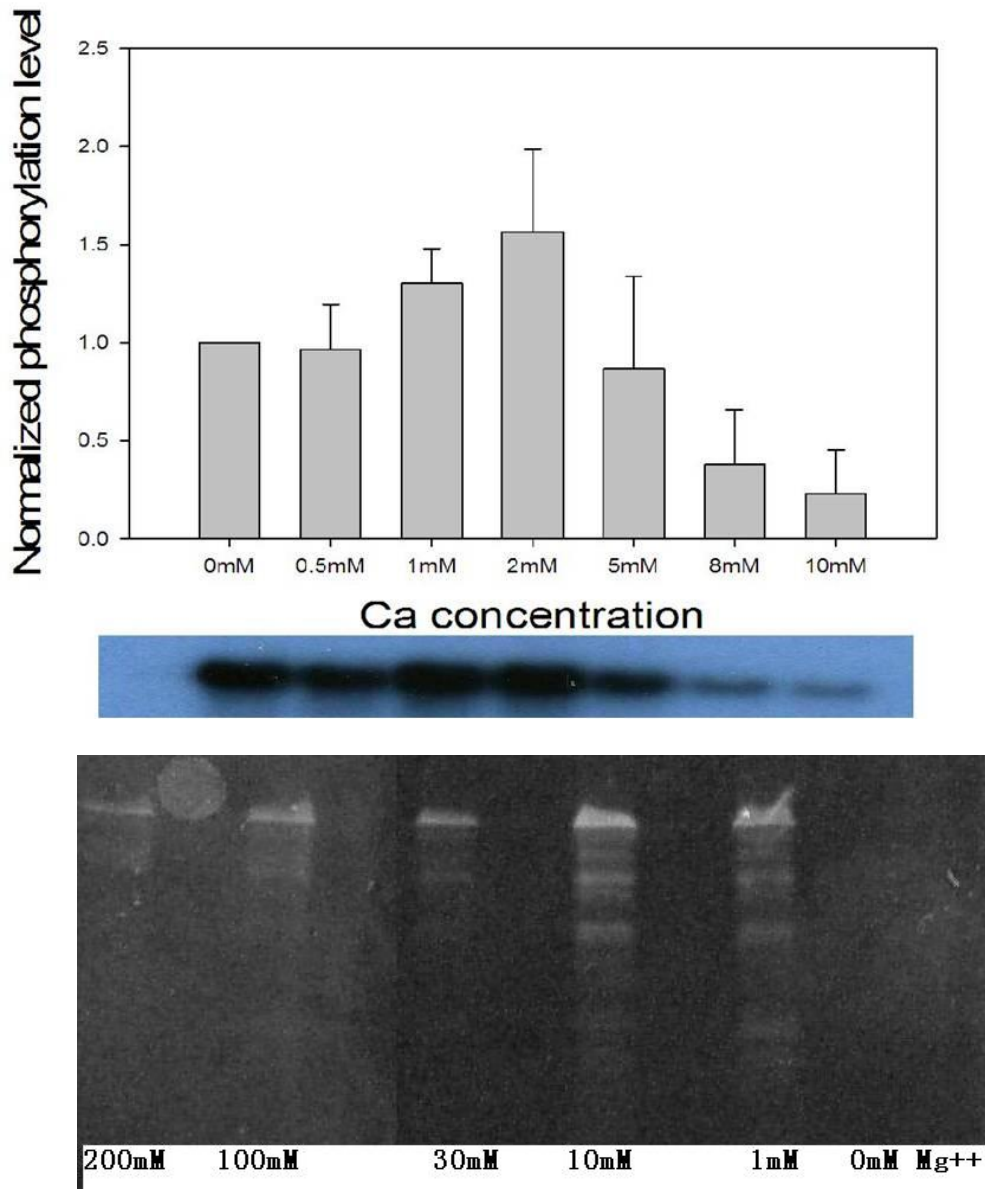


**Figure 19** In vitro phosphorylation of cDMP1 with different Ca<sup>2+</sup> (upper) or Mg<sup>2+</sup> concentration

The phosphorylation reaction was assessed at different calcium concentration, the increase of calcium, up to 2mM Ca<sup>++</sup> enhances the phosphorylation activity of CKI; if the calcium phosphorylation is >2mM then the phosphorylation activity was reduced. One way ANOVA suggests the phosphorylation level with 2mM Ca<sup>++</sup> is significantly higher (P= 0.08) compared to the group without Ca<sup>++</sup>. (Assessed by radiolabelled SDS-PAGE); At different magnesium concentration; the phosphorylation level increase between 1mM to 10mM, higher (>30mM) Mg<sup>++</sup> concentration inhibit the phosphorylation ability of the protein kinase. (Assessed by pro-Q stained SDS-PAGE)

Determination of protein phosphorylation by Mass spectrometry is a challenging technique. ESI (Electro spray ionization) is usually a more sensitive method than MALDI (Matrix-assisted laser desorption/ionization). This is due to the weak signal from phospho-peptides; it is difficult to obtain good ms/ms spectra using MALDI. On the other hand one advantage of the ESI method is that the phospho-peptides are separated from other peptides by using Liquid Chromatography prior to detection, which reduce the interference from the large excess of other peptides and enrich for the phospho-peptides. ESI has also some shortcomings, 1) large phospho-peptides are not easily eluted from the LC column 2) small phospho-peptides are eluted very early with salt which largely compromised the quality of MS spectra 3)  $H_3PO_4$  is easily lost in ion trap of any MS machine, which makes it more difficult to identify the phospho-sites.

In our experiment, we combined both MALDI and ESI to obtain more phospho-peptide information. Data from 4700(MALDI, CID) mass spectrometry analysis of cDMP1 phosphorylated by CKI show 6 phospho-peptides (Figure 20, Table 5); data from LTQ-XL (ESI, ETD) (Figure 21) and LCQ-Deca-xp (ESI, CID) (Figure 22) confirmed some of these phospho-peptides and also identified Ser66 as phospho-serine (Figure 22).

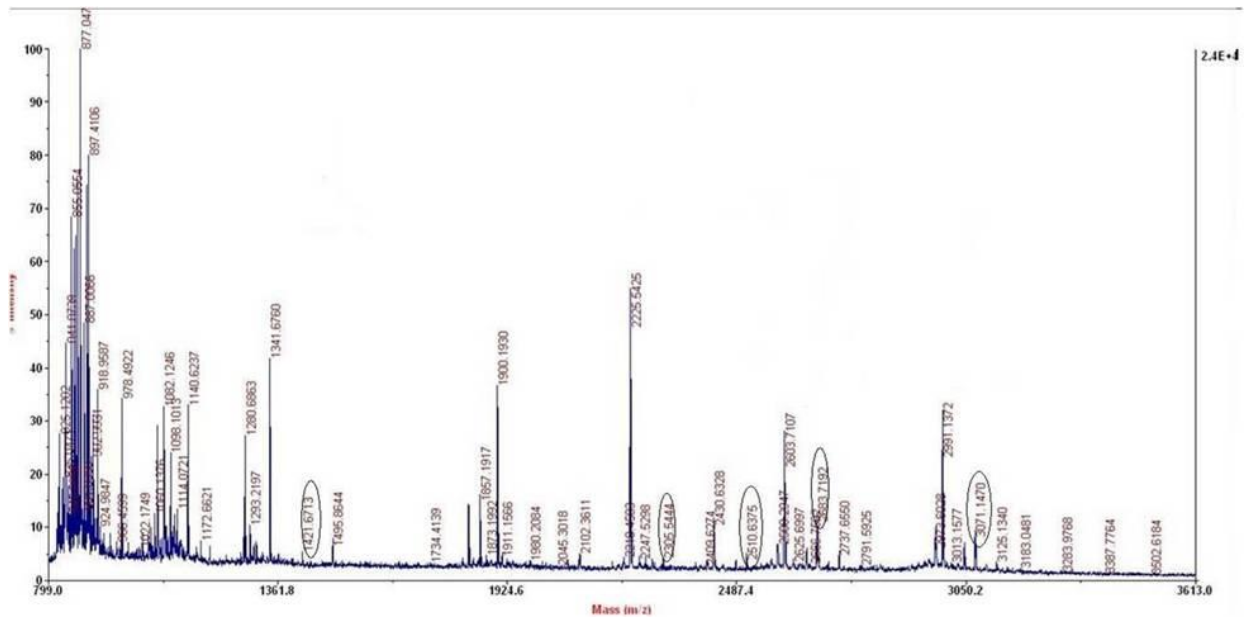


**Figure 20** MS of phosphorylated cDMP1 (phospho-peptides circled)

4700 mass spectrometry analysis detected 6 phospho-peptied (circled in Figure 20 and listed in Table 5) from cDMP1 phosphorylated by CKI.

**Table 5** Phospho-peptide of in vitro phosphorylated cDMP1 detected by MS

(M-MALDI, E-ESI)

Sequence	mass	position	Method	Missed cleavage
SEEDSDSQDSSR	1341.5037	252-263	M	0
SKEESNSTGSASSSEEDIRPK	2225.0164	264-284	M	1
GDREPTSTQDSDDSQ <b>S</b> VEFSSR	2430.0287	51-72	M,E	1
SQESQSEQDSRSEEDSDSQDSSR	2603.0208	241-263	M,E	1
SEESKGDREPTSTQDSDDSQ SVEFSSR	2990.2729	46-72	M,E	2
SESQEDTAESQSQEDSPEGQ DPSSESSEEAGEPSQESSE SQEGVTSESR	5264.0780	113-162	M	0



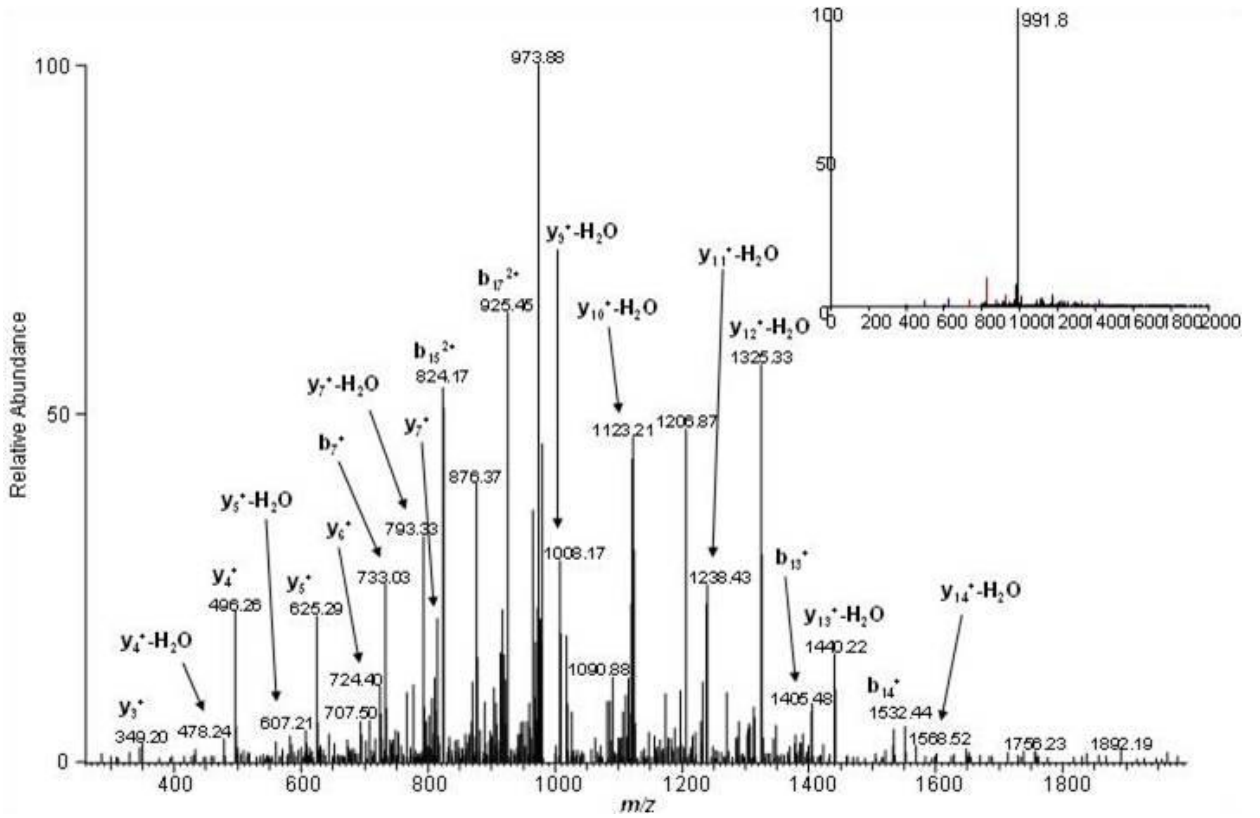


**Figure 21** Phosphor-peptide 3071(1023.85\*3) by LTQ-ESI MS<sup>n</sup>

(Upper right) MS<sup>2</sup> of a peptide ion at  $m/z$  1023.85 – little in terms of fragmentation information due to the predominant neutral loss of  $H_3PO_4$ . Neutral Loss Dependent MS<sup>3</sup> – 991.8 is “re-selected” for fragmentation (i.e. MS/MS/MS) producing significant sequence information to identify: SEESKGDREPTSTQDSDDSQSVEFSSR.

XC 6.322, ions 52/126, count 1  
DTA for scan 742 , Precursor ion: 838.32, charge 3, mass type: average

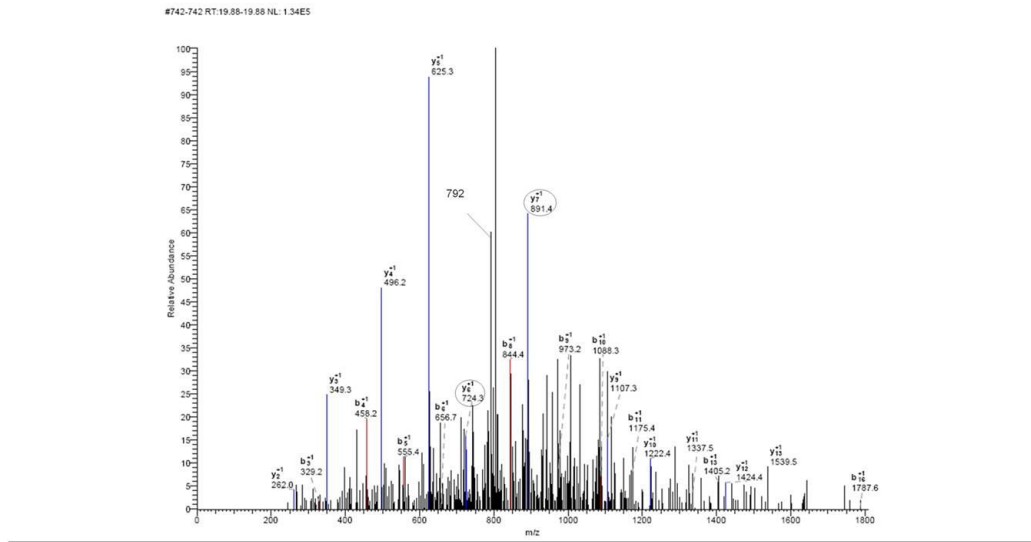


**Figure 22** Phospho-peptide 2510(838.32\*3) by LCQ-ESI MS<sup>2</sup>

Sequence identified: GDREPTSTQDSDSSQ**S**VEFSSR, y7(891.4) is a phospho-fragment while y6(724.3) is a non-phospho-fragment. 891.4 to 792 show a neutral loss of H<sub>3</sub>PO<sub>4</sub>.

## 4.5 ZYMOGRAM

Sequence analysis and previous studies have showed that CKII-like enzyme from the nucleus can phosphorylate DMP1; however, no direct identification of CKII was reported to date. Since we couldn't fully phosphorylate DMP1 using CKII in vitro, and considering the hierarchal

property of CKII, we hypothesized that CKII or other enzymes could phosphorylate DMP1 in vivo.

Firstly, we performed in vitro phosphorylation and confirmed that cellular fractions could phosphorylate cDMP1 (Figure 23). We collected cell lysates from MC3T3 (osteoblast), MDPC23 (odontoblast), NIH3T3 (fibroblast) and performed zymograms to find the corresponding enzyme band(s) that can phosphorylate DMP1. All 3 samples showed 3 bands exactly at the same positions (Figure 24). This zymogram experiment was repeated once. We concluded that there is no significant difference of kinases responsible for fDMP1 in mineralizing tissues versus non mineralizing tissues. At least 3 enzymes could phosphorylate fDMP1 in these cell lines, with molecular weight around 37, 40, and 60kDa, respectively. The radioactive bands were excised and analyzed by mass spectrometry; the lists of identified proteins included many protein kinases. DMP1 was also identified during the mass spectrometry analysis confirming that our digestion worked well. The 37kDa and 40kDa bands (because the gel is dried for imaging, it is hard to cut these two bands separately) have been analyzed by both 4700 MALDI-TOF and LTQ, while the 60kDa band was analyzed only by 4700. The total list of enzymes will be identified once we obtain the result of 60kDa band from LTQ.

CKII catalytic subunit alpha was identified in MC3T3 cell lysis corresponding to 5 peptides found, Figure 25, 26 show 2 ms/ms spectra of CKII subunit alpha peptides with high confidence. Although previous study[28] and sequence analysis suggested that CKII is the kinase that phosphorylate DMP1 in vivo, our research is the first direct evidence of CKII's involvement. We tested the following kinases: Cell division protein kinase 6 and cAMP-dependent protein kinase (only part of the sequence is available) for their ability to phosphorylate DMP1 but none of them showed this ability. The other kinases in the list were not commercially available.

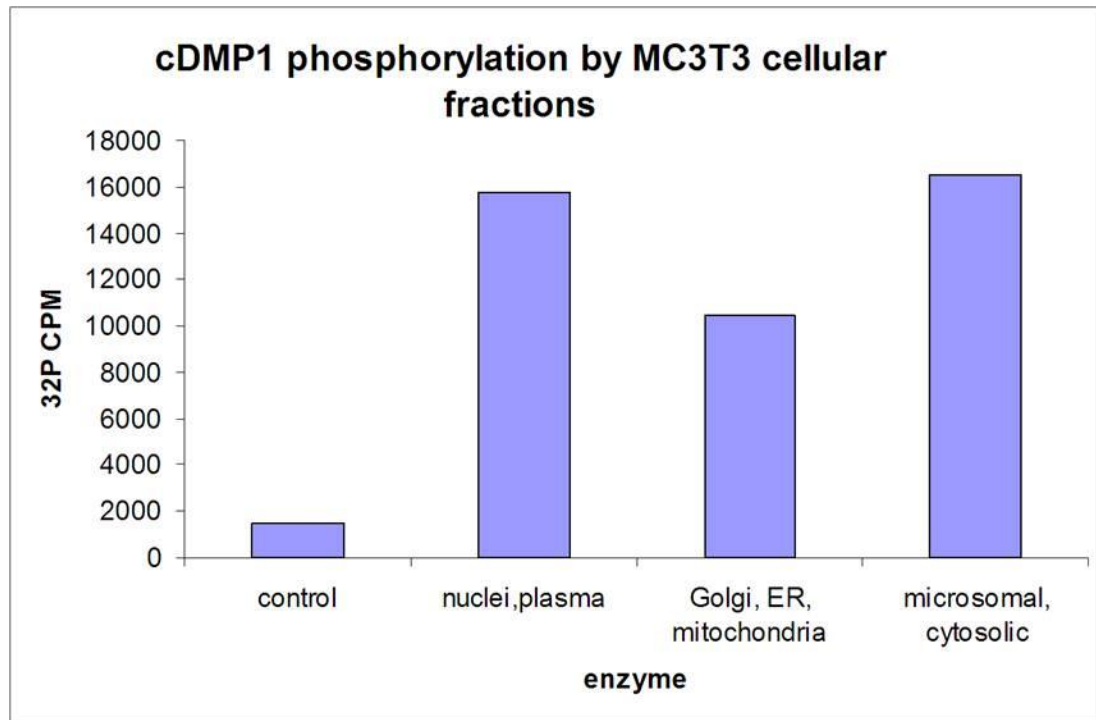


**Figure 23** cDMP1 phosphorylated by cellular fractions

In vitro phosphorylation confirmed that cellular fractions could phosphorylate cDMP1, the level is very low compared to CKI, the difference didn't mean the difference of phosphorylation level, but might only be experiments' error.

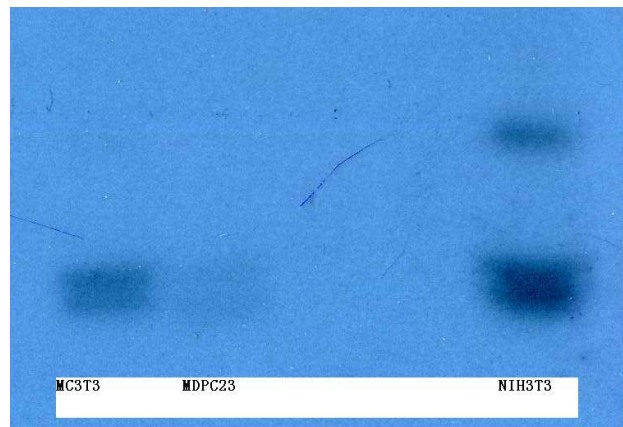
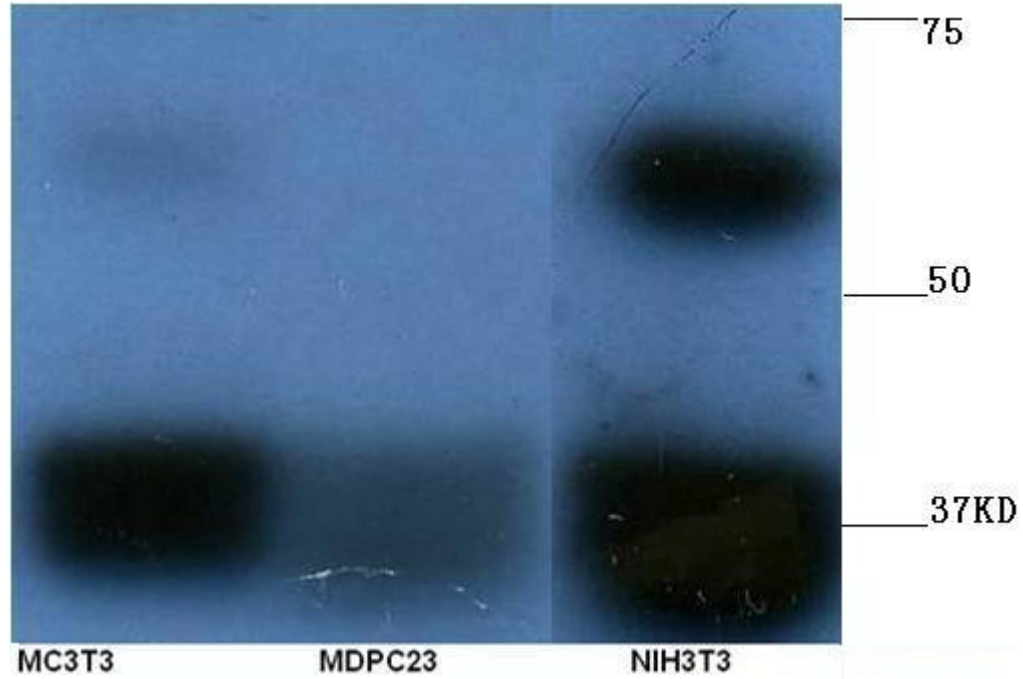


**Figure 24** fDMP1 zymogram bands

Upper panel: At least 3 bands were identified as being able to phosphorylate fDMP1 in these cell lines, with molecular weight around 37, 40, and 60kD. Lower panel: shorter exposure time picture to show the 2 bands.

**Table 6** List of kinases found in MC3T3 cell lysis' zymogram bands (37 and 40KD)

UniProt Acc	# of peptides	Protein
Q9Z1Z2	23	Serine-threonine kinase receptor-associated protein
Q9QZ08	17	N-acetyl-D-glucosamine kinase OS=Mus musculus
Q64261	6	Cell division protein kinase 6 OS=Mus musculus
Q80UL3	5	Galactokinase 1 OS=Mus musculus
O54833	5	Casein kinase II subunit alpha' OS=Mus musculus
Q8K183	4	Pyridoxal kinase OS=Mus musculus
P52332	3	Tyrosine-protein kinase JAK1 OS=Mus musculus
Q61846	2	Maternal embryonic leucine zipper kinase, OS=Mus musculus
Q61526	2	Receptor tyrosine-protein kinase erbB-3 OS=Mus musculus
P52480-1	2	Isoform M2 of Pyruvate kinase isozymes M1/M2
P05132-1	2	Isoform 1 of cAMP-dependent protein kinase catalytic subunit alpha OS=Mus musculus
O09110-1	2	Isoform 2 of Dual specificity mitogen-activated protein kinase kinase 3 OS=Mus musculus

The analysis is using Sequest, whose algorithm is matching experimental peptide to known fragmentation patterns of theoretical peptides. The protein abundances or presence were determined by # of peptide identified (as in column 2). All proteins listed in this table have been confirmed by looking into their peptides' spectra (as in Figure 25, 26)

#3756-3756 RT:33.53-33.53 NL: 1.39E4

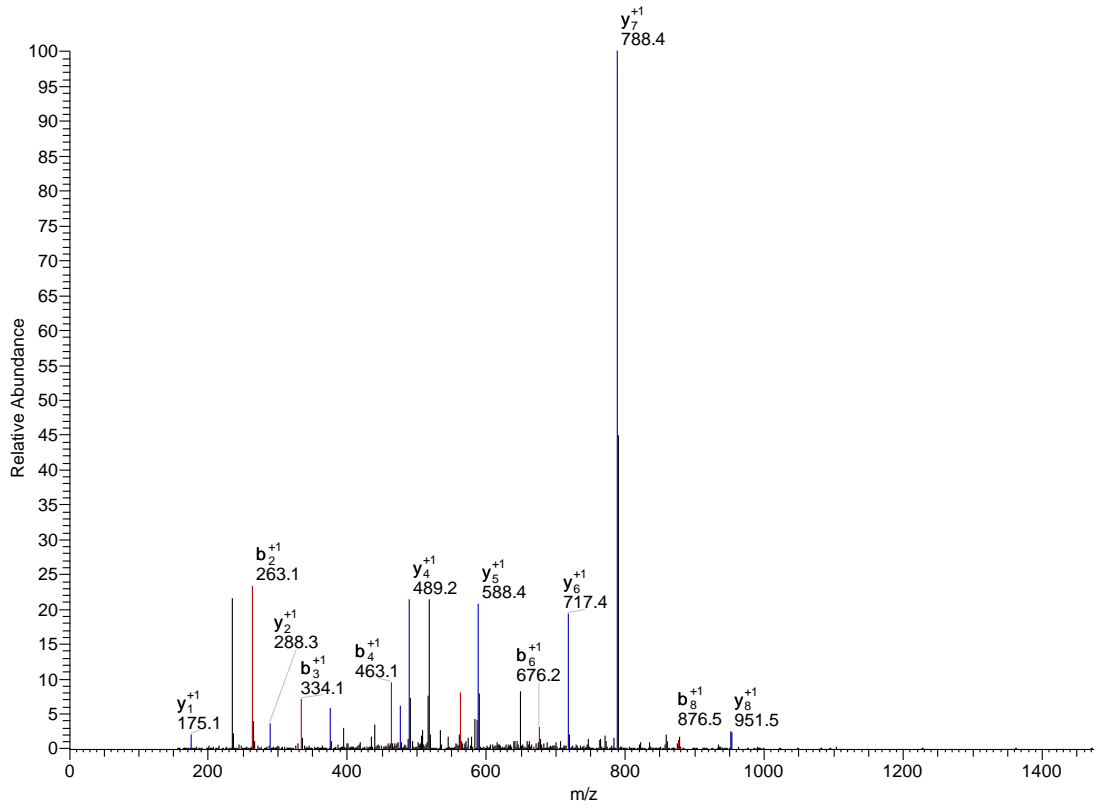


**Figure 25** MS/MS spectrum of peptide from CKII subunit alpha: VYAEVNSLR.

Ions series matched are labeled in red (b ions) or blue(y ions).

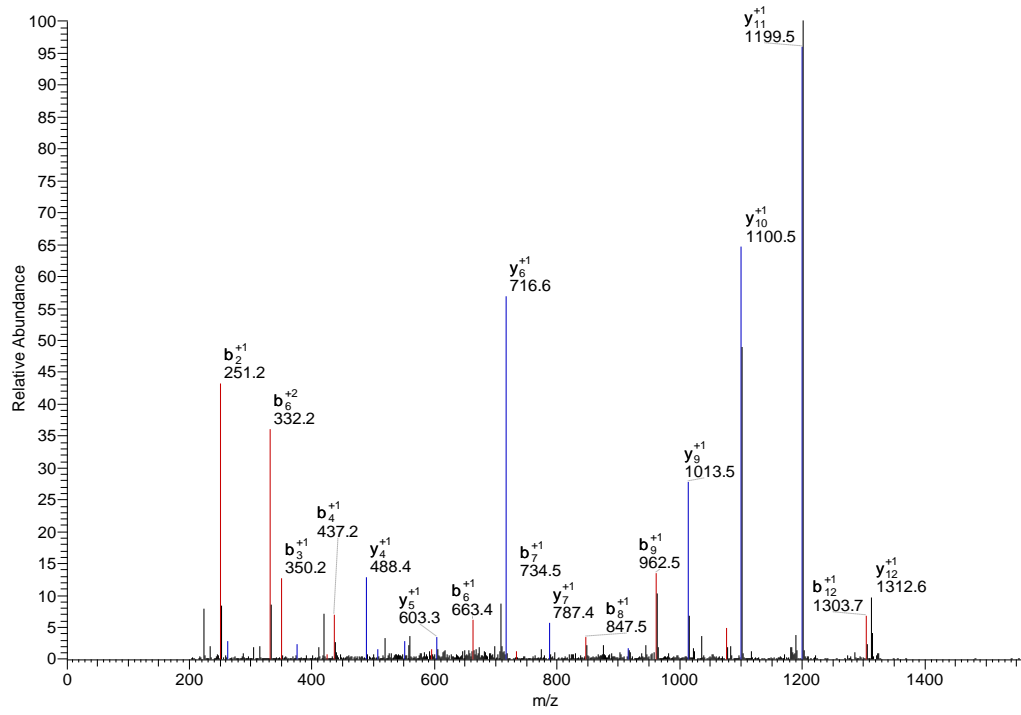


**Figure 26** MS/MS spectrum of peptide from CKII subunit alpha: HLVSPEALDLLDK

Ions series matched are labeled in red (b ions) or blue(y ions).



**Table 7** List of kinases found in MDPC23 cell lysis' zymogram bands(37 and 40KD)

UniProt Acc	# of peptides	Protein
P52480-1	49	Isoform M2 of Pyruvate kinase isozymes M1/M2 OS=Mus musculus GN=Pkm2
P09411	18	Phosphoglycerate kinase 1 OS=Mus musculus GN=Pgk1
P05132-1	4	Isoform 1 of cAMP-dependent protein kinase catalytic subunit alpha OS=Mus musculus
Q7TNL3-1	2	Isoform 1 of Serine/threonine-protein kinase 40 OS=Mus musculus
Q80UL3	2	Galactokinase 1 OS=Mus musculus
P20444	2	Protein kinase C alpha type OS=Mus musculus
P12382	2	6-phosphofructokinase, liver type OS=Mus musculus
Q61846	2	Maternal embryonic leucine zipper kinase
Q99N57-1	2	Isoform 1 of RAF proto-oncogene serine/threonine-protein kinase OS=Mus musculus
Q924C5	2	Alpha-protein kinase 3 OS=Mus musculus

The analysis is using Sequest, whose algorithm is matching experimental peptide to known fragmentation patterns of theoretical peptides. The protein abundances or presence were determined by # of peptide identified (as in column 2). All proteins listed in this table have been confirmed by looking into their peptides' spectra (as in Figure 25, 26)

#### 4.6 MAMMALIAN CELL DERIVED DMP1

Due to the high level of phosphorylation of DPP and DMP1, we hypothesized that the kinases present in mineralizing tissues such as bone and dentin would be different than the kinases present in non-mineralizing tissues. In order to compare the level of phosphorylation of DMP1 in mineralizing versus non mineralizing tissues, we over-expressed fDMP1 into cells that originated from mineralized tissues such as MC3T3 or U2OS cells or from connective tissue cells such as NIH3T3 or HEK-293 using an adenovirus that bare mouse fDMP1. We couldn't over-express DMP1 gene from NIH3T3 cells after trying several different conditions, which might indicate some degradation mechanism in fibroblast cells. MC3T3, U2OS, HEK-293 all are originated from tissues where DMP1 was found. The secreted DMP1 was purified by ion exchange (Figure 27) and confirmed by western blot (antibody from Dr. Qin). The comparison of DMP1 from MC3T3 versus HEK293 shows mostly similar but a little bit different cleavage and phosphorylation patterns (Figure 28). More 57kD and 37kD functional fragments were found in MC3T3 derived DMP1. DMP1 from U2OS, another bone derived cell was also phosphorylated. Our mass spectrum data (Figure 29-33) confirmed that we did purify DMP1 but did not provide phospho-peptide information from the cell derived fDMP1. This might be due to difficulty to detect phospho-peptide, or due to the possibility that phosphorylated amino acids are located in clusters which also occurs in OPN [29] and are hard to analyze by mass spectrometry.

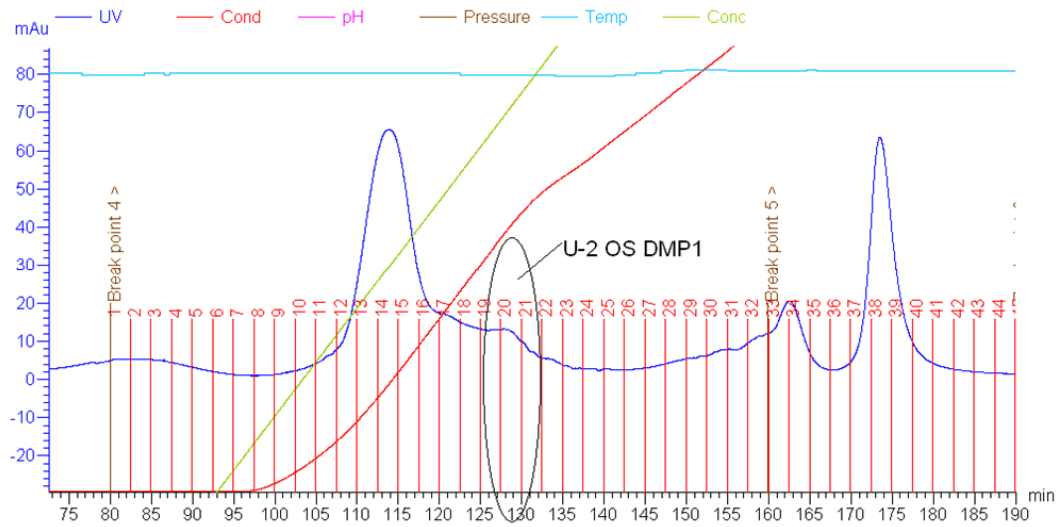


**Figure 27** U2OS derived fDMP1 purified by ion exchange.

U2OS derived fDMP1 was purified by ion exchange, the largest peak is FBS; the small peak circled is DMP1. Fractions 19-22 were collected.

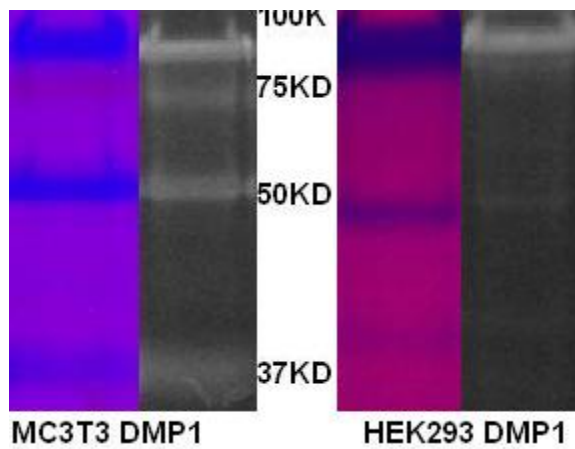


**Figure 28** MC3T3/ HEK293 derived DMP1 purified by ion exchange column

DMP1 purified from MC3T3 (left) and HEK293 (right) cell medium. The blue bands (stains-all) and bright bands (pro-Q stain) are DMP1. DMP1 from these two cell lines have mostly similar but a little bit different cleavage and phosphorylation patterns.

4700 Reflector Spec #1 MC=>BC=>AdvBC(32,0.5,0.1)->BC[BP= 1838.0,3039]

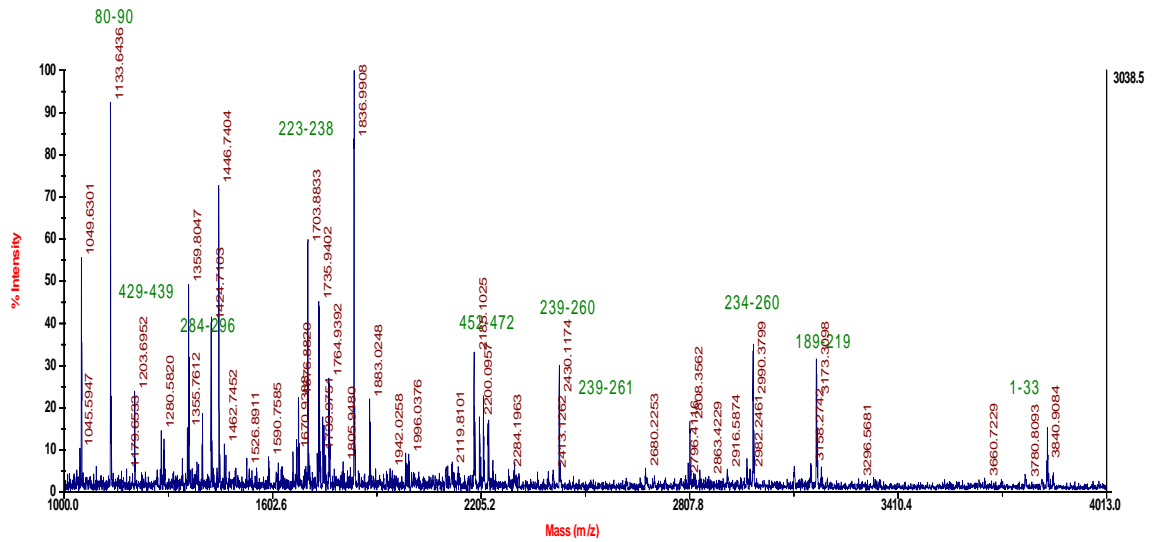
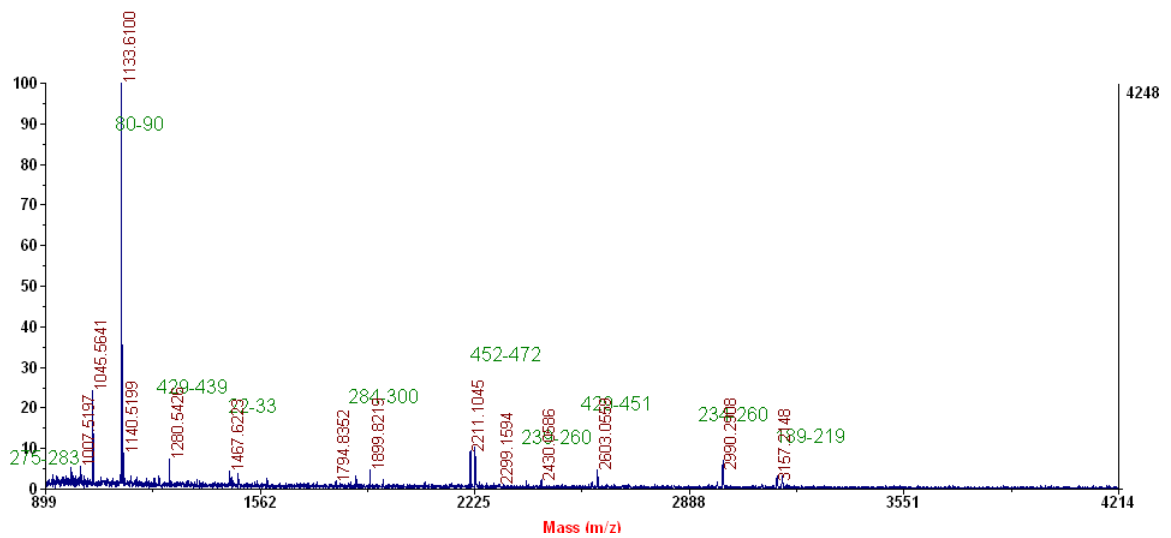


Figure 29 293 derived fDMP1 digested by trypsin. Coverage:31%

Identified peptide	Expected ms	Observed ms	Amino acid position
GQYRPAGGLSK	1133.6	1133.6	80-90
ETQSDSTEDTASK	1398.6	1398.7	429-439
ETQSDSTEDTASK	1398.6	1398.7	284-296
GHARMSSAGIRSEESK	1702.8	1703.8	223-238
SKEESNSTGSASSEDIRP K	2225.0	2225.1	452-472
GDREPTSTQSDSDSQSVEFS SR	2430.0	2430.1	239-260
SEESKGDREPTSTQSDSDSQ SVEFSSR	2990.3	2990.4	234-260
VGGGSEGESHHGDGSEFDDE	3173.2	3173.3	189-219
GM(O)QSDDPESTR			
MKTVILLVFLWGLSCALPVA	3778.9	3777.8	1-33
RYHNTESESSEER			



**Figure 30** U2OS derived fDMP1 digested by trypsin. Coverage:30%

Identified peptide	Expected ms	Observed ms	Amino acid position
GELTDSNSR	978.4	978.5	275-283
GQYRPAGGLSK	1133.6	1133.6	80-90
SQESQSEQDSR	1280.5	1280.5	429-439
YHNTESESSEER	1467.6	1467.6	22-33
ETQSDSTEDTASKEESR	1899.8	1899.8	284-300
SKEESNSTGSASSEEDIRP K	2225.0	2225.2	452-472
GDREPTSTQSDSDSVEFS SR	2430.0	2430.1	239-260
SQESQSEQDSRSEEDSDSQD SSR	2603.0	2603.0	429-451
SEESKGDREPTSTQSDSDSQ SVEFSSR	2990.2	2990.3	234-260
VGGGSEGESSHGDGSEFDDE	3157.2	3157.2	189-219
GMQSDDPESTR			

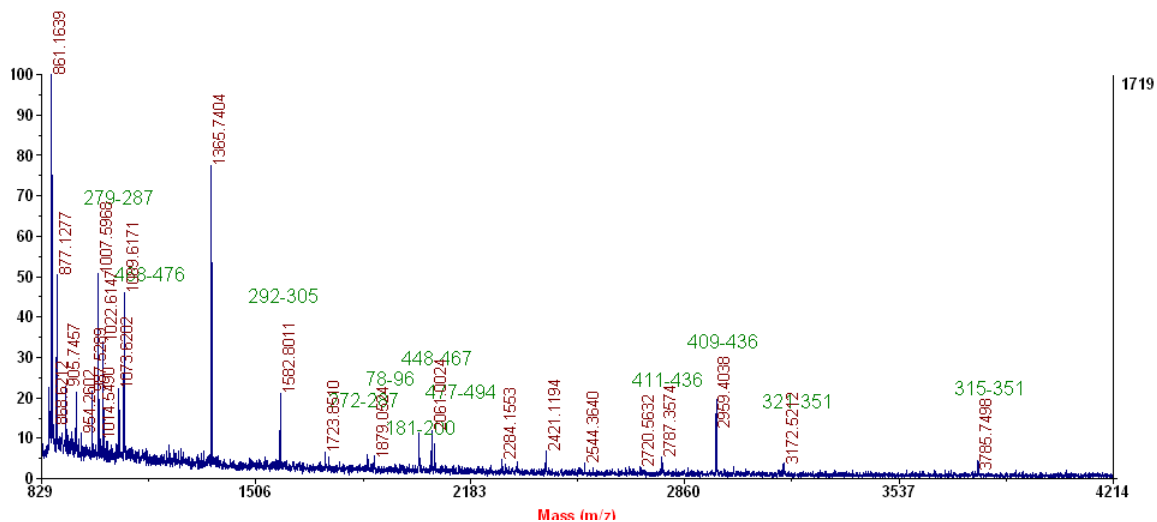


**Figure 31** U2OS derived fDMP1 digested by AspN. Coverage: 36%

Identified peptide	Expected ms	Observed ms	Aa position
DSNSRETQS	1023.4	1022.6	279-287
DIRPKNMEA	1073.5	1073.6	468-476
DTASKEESRSSEQE	1582.7	1582.8	292-305
DYRGELTDSNSRETQS	1857.8	1857.0	272-287
DRGQYRPAGGLSKSTGTGA	1878.9	1879.1	78-96
DSESEEQRVGGGSEGESSHG	2019.8	2020.0	181-200
DSSRSKEESNSTGSASSSEE	2060.8	2061.0	448-467
DSRKLIVDAYHNKPIGDQ	2069.1	2069.2	477-494
DSSSQEGLQSQSASTESRSQ ESQSEQ	2787.2	2787.4	411-436
DGDSSSQEGLQSQSASTESR SQESQSEQ	2959.2	2959.4	409-436
DPSESSEEEAGEPSQESSSE	3172.3	3172.5	321-351
SQEGVTSESRG			
DSPEGQDPSESSEEEAGEPS	3785.5	3785.7	315-351
QESSSESQEGVTSESRG			

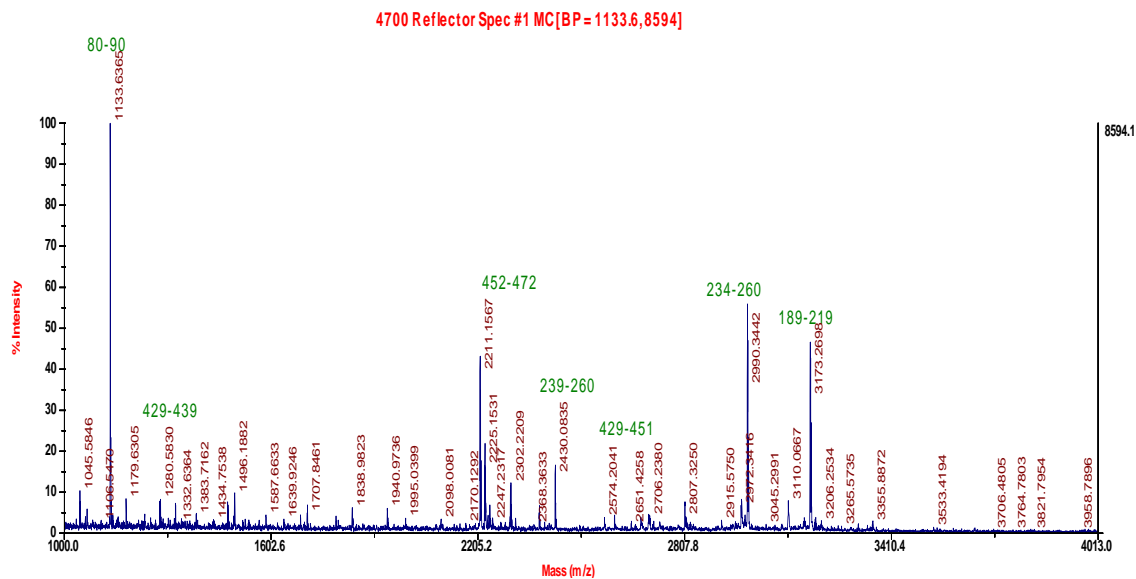


**Figure 32** MC3T3derived fDMP1 digested by Trypsin. Coverage:22%

Identified peptide	Expected ms	Observed ms	Amino acid position
GQYRPAGGLSK	1133.6	1133.6	80-90
SQESQSEQDSR	1280.5	1280.6	429-439
SKEESNSTGSASSSEDIRP K	2225.0	2225.2	452-472
GDREPTSTQSDSDSVEFS SR	2430.0	2430.1	239-260
SQESQSEQDSRSEEDSDSQD SSR	2603.0	2603.1	429-451
SEESKGDREPTSTQSDSDSQ SVEFSSR	2990.3	2990.3	234-260
VGGGSEGESSHGDGSEFDDE	3173.2	3173.3	189-219
GM(O)QSDDPESTR			

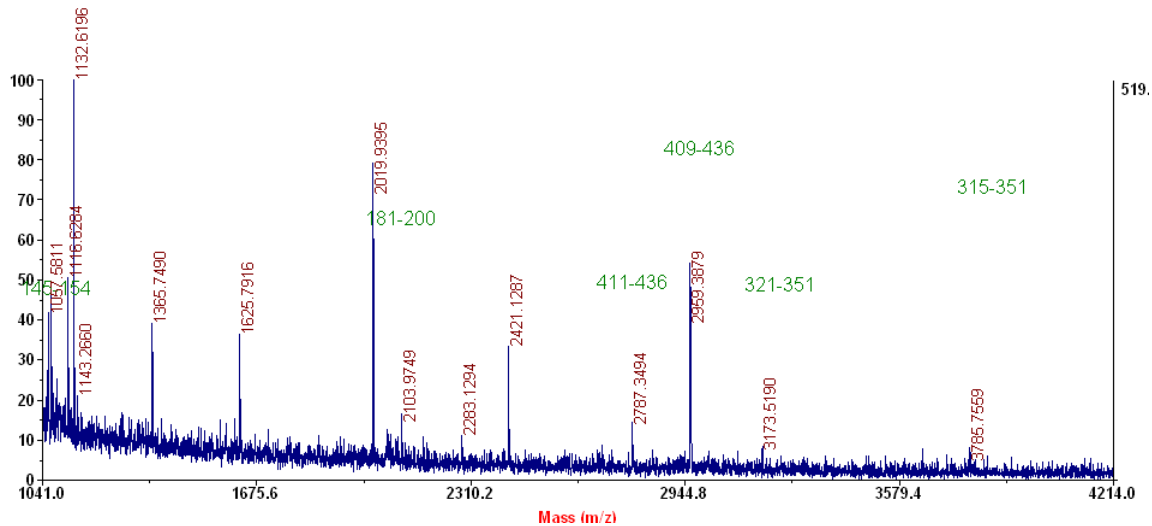


**Figure 33** MC3T3derived fDMP1 digested by AspN. Coverage: 19%

Identified peptide	Expected ms	Observed ms	Amino acid position
DTSQENSAQ	1066.4	1066.1	145-154
DSESEEQRVGGGSEGESSHG	2019.8	2019.9	181-200
DSSSQEGLQSQSASTESRSQ ESQSEQ	2787.2	2787.3	411-436
DGDSSSQEGLQSQSASTESR SQESQSEQ	2959.2	2959.4	409-436
DPSESSEEEAGEPSQESSSE	3172.3	3172.5	321-351
SQEGVTSESRG			
DSPEGQDPSESSEEEAGEPS	3785.5	3785.8	315-351
QESSSESQEGVTSESRG			

## 4.7 DISCUSSION

Osteoblast cells are a rich source of CKI and CKII activity[30], CKII was thought to be responsible for the phosphorylation of DPP[31] and DMP1 [28] from assays using CKII inhibitor,



however, no direct evidence has shown CKII's involvement. Our zymogram data identified CKII subunit from cell lysates and confirms CKII's role. Our data also shows that CKI can in vitro phosphorylate DDP and DMP1 much better than CKII. More attention should be dedicated to CKI's role in mineralized tissues. Unphosphorylated DMP1 was shown to first localize in the nucleus, works as regulator of osteoblast-specific genes [32], during maturation transition of the osteoblast, DMP1 was shown to get phosphorylated and migrate to the extracellular matrix [28], correspondingly, our data shows nuclei fraction from MC3T3 cell lysates do have the ability to phosphorylate DMP1. Under maturation transition conditions, the cells release calcium from their intracellular stores[33], and the export of DMP1 was found to be in response to the stimulus from  $Ca^{++}$ , which might be transported through IP3/ryanodine receptors[34]. Our results further confirm the role of  $Ca^{++}$  by showing different phosphorylation levels corresponding to different  $Ca^{++}$  concentration.

Phosphorylation level of DMP1 is important for its function. The 57kD fragments of highly phosphorylated DMP1 works as a hydroxyapatite nucleator, while low level of phosphorylation of DMP1 has no effect on either hydroxyapatite proliferation or growth[35]. Although published data suggest CKII was the enzyme responsible for DMP1[28], CKII could only phosphorylate DMP1 to a very low level (5 phosphate per DMP1) in vitro which couldn't function as mineral nucleator[35]. Despite the difference in the in vitro vs. the cell phosphorylation, we hypothesized that there might be other kinases participating in DMP1 phosphorylation. Our zymogram data not only provided the list of possible novel kinases, but also showed similar kinases pattern of both MC3T3 and NIH3T3 cells, which emphasized that it is might not the kinase specificity but the regulation mechanism (e.g, Calcium flux[28]) which differ the DMP1's phosphorylation and function.

## 4.8 SUMMARY AND FUTURE RESEARCH

We successfully phosphorylated DMP1 and DPP in vitro. When DMP1 was phosphorylated with CKI at 30°C for 1 hour, we were able to quantify approximately 13 phosphates per molecule. It was difficult to quantify DPP's phosphorylation due to the low binding of DPP to P81 paper. However, DPP's phosphorylation level was higher compared to DMP1 when assessed by loading the phosphorylation reaction mix using radioactive  $^{32}\gamma$ [ATP] onto an SDS-PAGE gel. Different conditions (temperature, time points, Ca<sup>2+</sup>/Mg<sup>2+</sup> ion concentration, enzymes) were assayed and we could obtain different phosphorylation level of DPP/DMP1 by adjusting these conditions. When DMP1 was in vitro phosphorylated by CKI at 30°C for 1 hour, we detected 6 phosphopeptides and identified Ser66 as a phosphorylation site by mass spectrometry.

We found there is no kinase specificity for DMP1 phosphorylation in mineralizing or non-mineralizing tissues, at least 3 different (forms) enzymes from cell lysate were responsible for DMP1 phosphorylation, with molecular weights of 37kD, 40kD and 60kD, respectively. CKII catalytic subunit alpha was identified, which is the first direct evidence of CKII's involvement in DMP1 phosphorylation. Some other possible novel kinases were identified from zymogram analysis, but most of them are not commercially available. Further research may focus on purifying and confirming these kinases.

Cell derived phosphorylation were compared by over-expressing and purifying DMP1 from mineralized and connective tissue cells. We couldn't over-express DMP1 gene from NIH3T3 cells after trying several different conditions, perhaps in fibroblast cells there might be some degradation mechanism to eliminate proteins that can initiate mineralization. We were able to purify DMP1 from MC3T3, U2OS, HEK-293 cells, which are originated from tissues where DMP1 was found. Comparison of MC3T3 and HEK293 derived DMP1 show similar cleavage

and phosphorylation pattern; however, there seems to be more 37kD and 57kD fragments in MC3T3 derived DMP1 compared with HEK293; these fragments were functionally active while the whole DMP1 is inactive. [25] This might indicate the difference of corresponding proteinase activity regulated by mineralized and connective tissue cells. Due to the limitation of mass spectrometry to analyze phospho-clusters, the phosphate analysis and localization remain a challenge from cell derived DMP1; we will use Inductively Coupled Plasma (ICP) to quantify the phosphate of these cell derived DMP1 and further analyze their role in mineralization.

Finally, we believe that the outcomes of this research will provide the basis to further assess the role of phosphorylation in mineralization.

## BIBLIOGRAPHY

1. Boivin, G. and P.J. Meunier, *Effects of bisphosphonates on matrix mineralization*. J Musculoskelet Neuronal Interact, 2002. **2**(6): p. 538-43.
2. Lowenstam, H.A., *Minerals formed by organisms*. Science, 1981. **211**(4487): p. 1126-31.
3. NIAMS, *Scientists Gain New Clues to Bone Mineralization*, in *Spot light on research*. 2006.
4. Satoyoshi, M., et al., *Extracellular processing of dentin matrix protein in the mineralizing odontoblast culture*. Calcif Tissue Int, 1995. **57**(3): p. 237-41.
5. Kadler, *collagen fibril formation*. Biochemical Journal, 1996. **316**.
6. Landis, *Mineral Deposition in the Extracellular Matrices of Vertebrate Tissues: Identification of Possible Apatite Nucleation Sites on Type I Collagen*. cells tissues organs, 2009. **189**: p. 20-24.
7. Termine, *Osteonectin, a bone-specific protein linking mineral to collagen*. Cell, 1981.
8. Prince, *Isolation, characterization and biosynthesis of a phosphorylated glycoprotein from rat bone*. J Bio Chem, 1987. **262**.
9. George, *Characterization of a novel dentin matrix acidic phosphoprotein*. J Bio Chem, 1993. **268**.
10. Veis, *The biosynthesis of phosphophoryns and dentin collagen in the continuously erupting rat incisor*. J Bio Chem, 1978. **253**: p. 6845-6852.
11. Fisher, L.W. and N.S. Fedarko, *Six genes expressed in bones and teeth encode the current members of the SIBLING family of proteins*. Connect Tissue Res, 2003. **44 Suppl 1**: p. 33-40.
12. Rowe, P.S., et al., *MEPE, a new gene expressed in bone marrow and tumors causing osteomalacia*. Genomics, 2000. **67**(1): p. 54-68.
13. Pinto, M.R., et al., *Age-related changes in composition and Ca<sup>2+</sup>-binding capacity of canine cortical bone extracts*. Am J Physiol, 1988. **255**(1 Pt 2): p. H101-10.
14. Veis, *Non-collagenous proteins of bone and dentin Extracellular matrix*. Chap. in Calcium Binding proteins and Calcium functions. 1977: North Holland:Elsevier.
15. George, *Role of phosphophoryn in Dentin Mineralization*. cells tissues organs, 2005. **181**(No. 3-4).
16. Evans, J.S., T. Chiu, and S.I. Chan, *Phosphophoryn, an "acidic" biomineralization regulatory protein: conformational folding in the presence of Cd(II)*. Biopolymers, 1994. **34**(10): p. 1359-75.
17. Lee, S.L., T. Glonek, and M.J. Glimcher, *<sup>31</sup>P nuclear magnetic resonance spectroscopic evidence for ternary complex formation of fetal dentin phosphoprotein with calcium and inorganic orthophosphate ions*. Calcif Tissue Int, 1983. **35**(6): p. 815-8.
18. Qin, C., O. Baba, and W.T. Butler, *Post-translational modifications of sibling proteins and their roles in osteogenesis and dentinogenesis*. Crit Rev Oral Biol Med, 2004. **15**(3): p. 126-36.
19. Yamakoshi, Y., et al., *Dentin sialophosphoprotein is processed by MMP-2 and MMP-20 in vitro and in vivo*. J Biol Chem, 2006. **281**(50): p. 38235-43.

20. Yamakoshi, Y., *Dentin Sialophosphoprotein and Dentin*. J. Oral Biosci, 2008. **50**: p. 33-44.
21. Feng, J.Q., et al., *Generation of a conditional null allele for Dmp1 in mouse*. Genesis, 2008. **46**(2): p. 87-91.
22. Narayanan, K., et al., *Differentiation of embryonic mesenchymal cells to odontoblast-like cells by overexpression of dentin matrix protein 1*. Proc Natl Acad Sci U S A, 2001. **98**(8): p. 4516-21.
23. Feng, J.Q., *Dentin matrix protein 1, a target molecule for Cbfa1 in bone, is a unique bone marker gene*. J Bone Miner Res, 2002. **17**: p. 1822-1831.
24. Qin, C., R. D'Souza, and J.Q. Feng, *Dentin matrix protein 1 (DMP1): new and important roles for biomineralization and phosphate homeostasis*. J Dent Res, 2007. **86**(12): p. 1134-41.
25. Qin, C., et al., *Evidence for the proteolytic processing of dentin matrix protein 1. Identification and characterization of processed fragments and cleavage sites*. J Biol Chem, 2003. **278**(36): p. 34700-8.
26. Graves, P.R.a.R., P.J., *Role of COOH-terminal Phosphorylation in the Regulation of Casein Kinase I*. J. Biol. Chem, 1995. **270**: p. 21689-21694.
27. *technical reference for products*, New England Biolab.
28. Narayanan, K., et al., *Dual functional roles of dentin matrix protein 1. Implications in biomineralization and gene transcription by activation of intracellular Ca<sup>2+</sup> store*. J Biol Chem, 2003. **278**(19): p. 17500-8.
29. Christensen, B., et al., *Post-translationally modified residues of native human osteopontin are located in clusters: identification of 36 phosphorylation and five O-glycosylation sites and their biological implications*. Biochem J, 2005. **390**(Pt 1): p. 285-92.
30. Wu, C.B., S.L. Pelech, and A. Veis, *The in vitro phosphorylation of the native rat incisor dentin phosphophoryns*. J Biol Chem, 1992. **267**(23): p. 16588-94.
31. Sfeir, C. and A. Veis, *The membrane associated kinases which phosphorylate bone and dentin extracellular matrix phosphoproteins are isoforms of cytosolic CKII*. Connect Tissue Res, 1996. **35**(1-4): p. 215-22.
32. Narayanan, K., et al., *Dentin matrix protein 1 regulates dentin sialophosphoprotein gene transcription during early odontoblast differentiation*. J Biol Chem, 2006. **281**(28): p. 19064-71.
33. Lundgren, T., et al., *Junctional proteins and Ca<sup>2+</sup> transport in the rat odontoblast-like cell line MRPC-1*. Calcif Tissue Int, 2001. **68**(3): p. 192-201.
34. Adebajo, O.A., et al., *Novel biochemical and functional insights into nuclear Ca(2+) transport through IP(3)Rs and RyRs in osteoblasts*. Am J Physiol Renal Physiol, 2000. **278**(5): p. F784-91.
35. Tartaix, P.H., et al., *In vitro effects of dentin matrix protein-1 on hydroxyapatite formation provide insights into in vivo functions*. J Biol Chem, 2004. **279**(18): p. 18115-20.

